HUMBOLDT-UNIVERSITÄT ZU BERLIN

LEBENSWISSENSCHAFTLICHE FAKULTÄT

INSTITUT FÜR BIOLOGIE

MASTERARBEIT

ZUM ERWERB DES AKADEMISCHEN GRADES

MASTER OF SCIENCE

"Bedrohungswahrnehmungsmoment:
Konzeption, Entwurf und Implementierung einer neuartigen angstbasierten Verhaltensaufgabe"

“Threat perception moment:
conception, design and implementation of a novel fear-based behavioral task”

vorgelegt von

Marti Ritter

geb. am 30.08.1993 in Berlin

angefertigt in der Arbeitsgruppe Larkum

am Institut für Biologie

Berlin, im Juni 2020

First Reviewer: Prof. Dr. Matthew Larkum

Second Reviewer: Prof. Dr. Michael Brecht

Zusammenfassung

In dieser Masterarbeit werde ich die Konzeption, den Designprozess, und Implementierung eines neuartigen Setups beschreiben, welches genutzt werden kann, um die Hirn- und Verhaltensprozesse zu untersuchen, welche in der Verarbeitung einer nicht unmittelbar erkennbaren Bedrohungssituation beteiligt sind. Ich beginne mit einer kurzen Einführung in den derzeitigen Stand der Angstforschung, worauf eine Erklärung des Planungsprozesses hinter dem Design des implementierten Verhaltens folgt. Schlussendlich werde ich das Protokoll beschreiben, welches wir erwarten in der Erzeugung und Beurteilung der inhärenten Angst in Mäusen zu verwenden, und die Masterarbeit mit einem Ausblick auf die möglichen Anwendungsgebiete des Setups abschließen.

Abstract

In this master thesis, I will describe the concept, design process, and implementation of a novel setup, which can be used to research the neural and behavioral processes, involved in the processing of an ambiguous threat. Here I begin with a short introduction to the current state of research into fear, followed by an explanation of the thought process behind the design for the behavior that we have implemented, and finally I describe the protocol we expect to use in assessing and generating innate fear in mice. I will end with an outlook on the potential applications of the setup.

Table of contents

1. Introduction

Fear is a central emotion guiding the behavior of animals and people. Fight or flight, a standard behavioral outcome, is known to most of us as a reaction to threatening situations. The brain circuits that guide the display of fear, and the behavioral reaction to events that elicit fear have been extensively studied over the last decades (Tovote, Fadok, and Lüthi 2015; Silva, Gross, and Gräff 2016; LeDoux and Brown 2017). In fact, years of research show that brains have evolved to solve complex perceptual tasks, such as perceiving whether a stimulus is rewarding or threatening, in a modular fashion involving the cooperation of multiple areas of the brain. To understand how the brain functions to perceive fear and reacts to elements of the environment that can potentially be threatening, it is therefore necessary to dissect both the modular processes and the combined, brain-wide integration of these processes. The correct reaction to an ambiguous threat situation is a crucial element of survival. In this moment, the moment where a threat is perceived as a threat, the brain rapidly integrates many aspects of its current environment and evaluates them against a range of memories and internal expectations to finally decide on an appropriate reaction.

This moment, the threat perception moment (TPM), can best be understood by an example. Most people learn that they are safe in a zoo because the animals in a zoo are not threatening. For example, a nest of snakes that is behind a glass partition is not dangerous. A visitor to the zoo feels safe in the knowledge that the current context, being on the other side of a glass pane, is sufficient protection from the snakes. If the glass pane suddenly disappears or breaks, the visitor might scream, or try to run away or could be frozen in the middle of snakes. At a minimum, there would be a new context, a potential novel threat, to evaluate.

Here we have designed a behavioral apparatus to assess the sensory input, the brain's response to the new context, and the animal’s behavior during the assessment of the threat. We are interested in assessing how the cognitive and perceptual events lead to the moment when a threat is recognized, and how behaviors change when a threat is recognized. We will utilize innate fear, the mouse’s fear of rats, to generate this sudden and ambiguous threat. The understanding of these phenomena and the neural circuits that contribute to TPM will be important for neuroscience, and for understanding human phobias and fear-disorders. This master thesis will introduce a setup, which allows the simulation of this TPM.

2. Background (Literature review)

2.1 Fear as an emotion

is elicited by a threat or the expectation of a threat. It is one of the most basic feelings one could imagine, but it is hard to clearly define fear with a single moniker that includes and considers not only the subjective emotion of fear, which can currently be evaluated primarily in human beings, but also the underlying neural circuits and cortical processes, whose in-depth study is currently possible only in animals. This might be one of the reasons, why, since the beginning of aversive conditioning using threat as an unconditioned stimulus (Mowrer and Lamoreaux 1946) until today, there has been no agreed-upon definition of, or even clear distinction between 'fear' as an emotion and the associated behavioral responses (Fanselow and Pennington 2017; Mobbs et al. 2019). In recent times there have been attempts to address this and settle on a definition (Mobbs et al. 2019; Perusini and Fanselow 2015).

The neural basis of fear perception can be understood by breaking fear (threat) perception into its basic component circuits: the components involved in perceiving danger, those reacting to the threat, and then translating this threat into the appropriate behavior. There are multiple components activated in this process: a core circuit, which is active in all situations involving fear and threat and is probably involved in learning during the experience of innate fear (Silva, Gross, and Gräff 2016), and an additional circuits specific to particular sensory inputs, which detect the threat and integrate available information and, finally, output an appropriate reaction (Fanselow 1994; Mobbs et al. 2019). These responses can relate to the reaction of a mouse to a looming stimulus, associated with a flying predator, or the smell of a rat or cat, for example.

The main motivation of research into fear is the frequent occurrence of psychiatric pathologies associated with fear in humans (Flores et al. 2018): The average person in a developed country has a 30% chance to experience an anxiety or fear-based disorder in their lives (Kessler et al. 2012). Each year around 12% of the entire population is affected by such a disorder (Wittchen et al. 2011). These disorders also come with severe consequences in the form of a threefold increase in suicide-rate (Kanwar et al. 2013) and a high cost to the local economies due to work loss days, which are for some anxiety disorders higher than for common somatic disorders like diabetes (Bandelow and Michaelis 2015).

Even though the goal is to address how the threat perception moment occurs in human beings, it is currently not possible to perform experimental manipulations of the human brain or study the human brain at a subcellular resolution. The techniques used to study human brain circuits, like fMRI or EEG (Logothetis et al. 2001), or even single unit recording cannot achieve the spatiotemporal resolution. Furthermore, the paradigms involved in fear conditioning are not directly translatable to humans. For these reasons, it is necessary to develop and use animal models.

2.2 Circuits involved in fear, and their functions, are crucial to understanding the mechanisms involved in fearful behavior. Here I will introduce the structures involved in expressing fear and recognizing threats: the amygdala, insular cortex, and hippocampus.

Traditionally, these brain circuits have been studied in the context of Pavlovian fear conditioning, where the emotion of fear is induced by a conditioned stimulus. This work was mostly concerned with the question of how the brain learned about and reacts to threats (LeDoux 2014). Novel approaches in exploring circuits, both local microcircuits and long-range projection-specific pathways, have helped in identifying the elements involved in fear and anxiety (**Figure 1**) and understanding how the brain produces both (Tovote, Fadok, and Lüthi 2015).

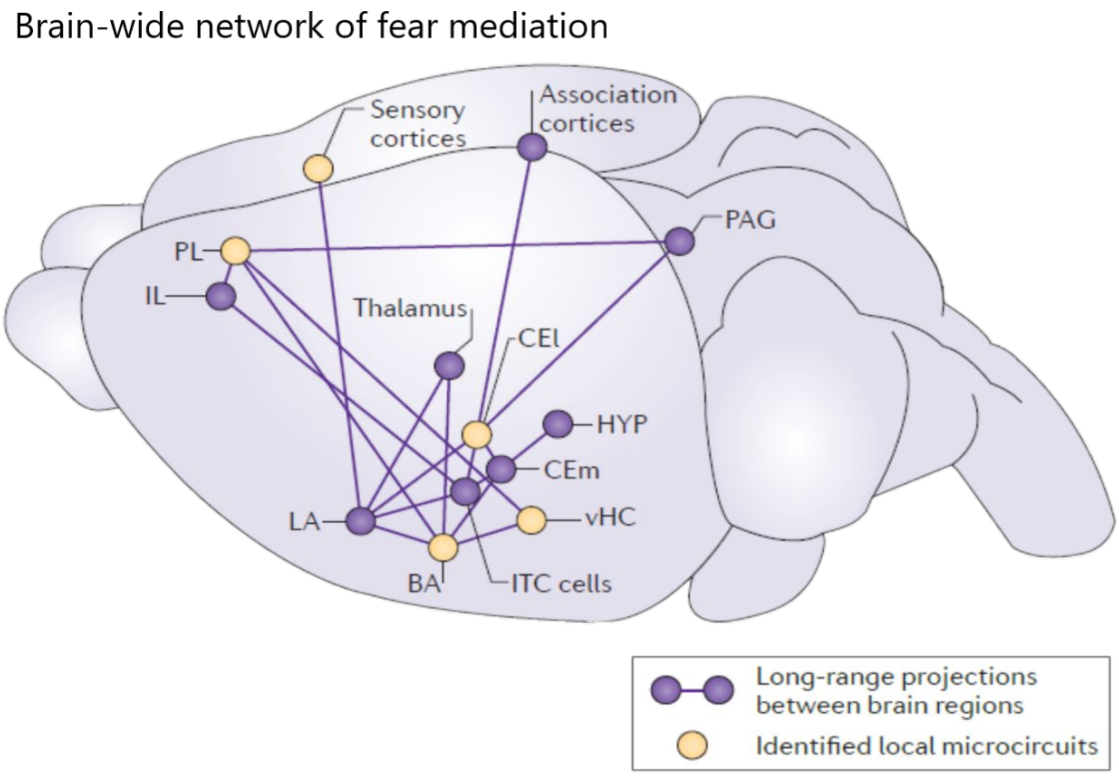

Figure 1 *Schematic image of brain-wide, long-range excitatory and inhibitory connections involved in mediating fear states. Many cortical (association cortices, sensory cortices, prelimbic cortex/PL, and infralimbic cortex/IL) and hippocampal (ventral hippocampus/vHC) areas are thought to be involved in mediating and expressing fear. In addition, many nuclei in the amygdala (lateral and medial central amygdala/CEl&CEm, basal amygdala/BA, lateral amygdala/LA), periaqueductal grey (PAG), thalamus and hypothalamus (HYP) are also involved in these behaviors. ITC – intercalated cells;*
Adapted from: Tovote, Fadok, and Lüthi 2015, Figure 1a

2.2.1 The amygdala

is a key brain region involved in associative learning of fear (Krabbe, Gründemann, and Lüthi 2018). The basolateral amygdala receives sensory input and funnels sensory information to the rest of the amygdala complex (**Figure 2**). Plasticity of the excitatory principal neurons in this area plays a crucial role in learning conditioned fear responses (Krabbe, Gründemann, and Lüthi 2018).

Nearly 70 years ago, the amygdala was already thought to be involved in defensive responding, mostly in the form of growling in cats (de Molina and Hunsperger 1959). This was studied with large amplitude, short duration electrical stimulation of multiple brain areas, including the central nucleus, where stimulation of the amygdala elicited defensive behavior (de Molina and Hunsperger 1959). In addition to this function, the Amygdala has also been shown to be involved in appetitive responses to potential food-sources (Gallagher, Graham, and Holland 1990). The central amygdala has been found to have long-range connections with the gustatory section of the insular cortex, another region involved in fear, and these connections, in addition to the connectivity with the lateral division of the central nucleus create excitatory monosynaptic connections with distinct populations of neurons in the central nucleus (H. C. Schiff et al. 2018). Manipulation of these connections modifies the ability of the animal to establish taste-reinforced behavioral responses (H. C. Schiff et al. 2018).

2.2.2 The insular cortex

has also been identified as a potential site for threat/safety-estimation and -integration, including the reaction to learned safety signals that inhibit fear (Foilb et al. 2016). The reduction of fear responses to threat signals, during the simultaneous detection of safety signals, is termed conditioned inhibition of fear. Injections of a NMDA-receptor antagonist into the posterior insular cortex before training prevented inhibition learning in a conditioned fear paradigm. The effect was specific to the posterior insula (there was minimal effect of injections into the anterior and medial insular cortex showed no effect (Foilb et al. 2016). These results suggest that the insular cortex in addition to the amygdala may have a role in danger expectation (Foilb et al. 2016).

In another recent study, it was found that multimodal inputs that converge in the posterior insular cortex then project to subcortical targets involved in emotional and motivational mediation. Manipulation of these circuits results in a reduction in exploration and feeding in reaction to bodily and affective adversity, hinting at multiple facets of aversive states being mediated in subcortical projections of the posterior insular cortex (Gehrlach et al. 2019). Yet there have been appetitive regions found in the more anterior sites of the insular cortex (Peng et al. 2015; Castro and Berridge 2017), which raises the questions whether there are topographically distinct sections in the insular cortex which represent positive internal states and, if they exist, whether they interact with the posterior sections (Gehrlach et al. 2019).

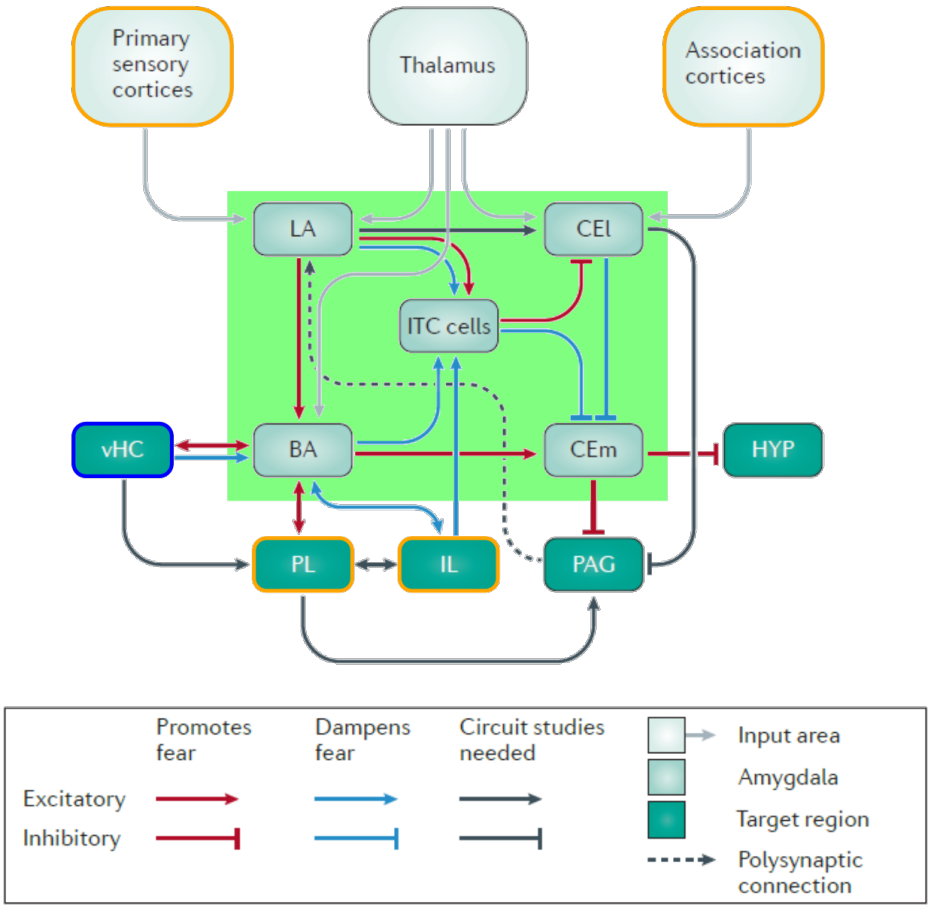

Figure 2 *Input and output projections of amygdala nuclei.*
Multiple areas in the amygdala receive cortical and thalamic input and show high levels of fear-related neuronal activity. This graphic emphasizes the prelimbic cortex (PL) and the ventral hippocampus (vHC) connections to the basal amygdala (BA) which modulate the long-term changes in activity, i.e. plasticity. Central nuclei of the amygdala promote fear behavior by projecting to hypothalamic and brainstem centers. Extinction of fear is controlled by the same structures, using different circuit elements. Fear output from the lateral central amygdala (CEl) to the hypothalamus (HYP) and the periaqueductal gray (PAG) is dampened by projections from the infralimbic cortex (IL) to the BA and to the intercalated cells (ITC). There are still open questions regarding identity, connectivity, and function of forebrain-to-brainstem fear pathways.
Legend: orange – cortical areas; green – amygdala; blue – hippocampus
Adapted from: Tovote, Fadok, and Lüthi 2015, Figure 1b

2.2.3 The hippocampus' role in fear conditioning and expression is complex. It is not involved in fear itself, but rather in the learning of complex conditioned learning (Phillips and LeDoux 1992, **Figure 3**). For example, when rats are conditioned to an auditory cue associated with a foot shock, lesions of the hippocampus decreased fear responses during the time before the conditioned stimulus was presented (Phillips and LeDoux 1992). Lesions of the amygdala on the other hand, affect fear responses during the presentation of the conditioned stimulus and before the presentation of this stimulus. This ability to integrate contextual information is not compromised during behaviors in virtual environments (Harvey et al. 2009; Dombeck et al. 2010).

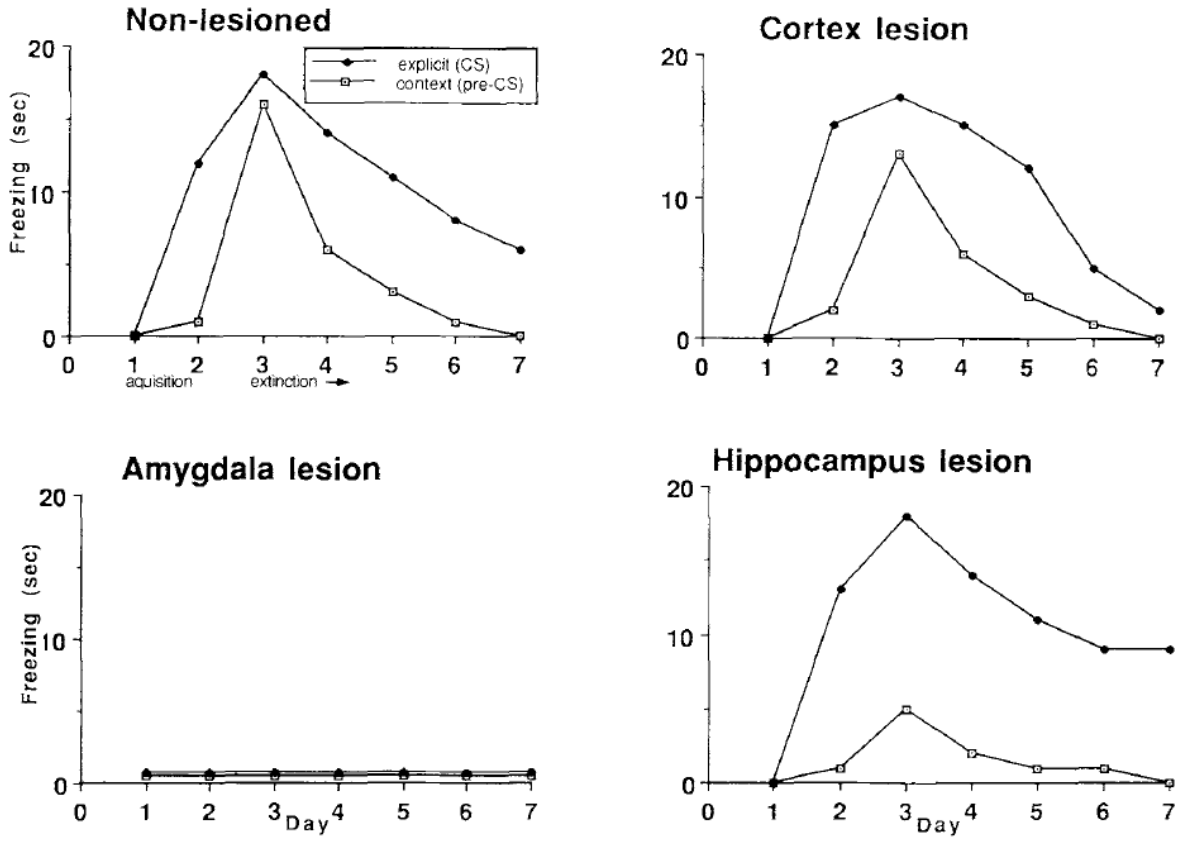

Figure 3 *Effects of amygdala and hippocampus lesions on the fear-response.*
Control rats were conditioned by presenting a tone (conditioned stimulus, CS) followed by a short shock (unconditioned stimulus, US). Context was established by performing the conditioning in the same rodent conditioning chamber for multiple days. The rate of freezing during the time window before the presentation of the conditioned stimulus (context, pre-CS) was used to measure the level of contextual fear conditioning, while the rate of freezing during the presentation of the conditioned stimulus was used to measure cued fear conditioning (explicit, CS).
Lesions were made in the cortex, amygdala, and hippocampus, by passing an anodal constant current through an electrode and animals were trained in the same behavioral paradigm as the control animals. It was shown that the amygdala-lesioned rats showed little to no freezing during the experiment, even after multiple days. Hippocampus-lesioned rats on the other hand showed the normal pattern of freezing during the presentation of the CS, but very little freezing during the context period before the presentation. Finally, cortical lesions did not appear to influence the freezing behavior, as the cortex-lesioned rats showed the same freezing pattern as the unoperated controls.
Adapted from: Phillips and LeDoux 1992, Figure 2

2.3 Innate fear

encompasses all types of fear associated with inherently negative or aversive stimuli. Fear can be categorized as innate or learned. Innate fear is associated with unconditioned stimuli, while learned fear originates from memories associated with conditioned stimuli. There are distinct neural circuits and pathways for each kind of fear. In the case where innate and learned fear co-occur, innate fear dominates and overrides the learned response (Isosaka et al. 2015).

The behavioral reaction to unconditioned stimuli occurs naturally: they elicit a defensive response but are not necessarily learned. Pathways for processing and estimating the danger vary with the type of stimulus that elicits fear. There are known pathways for predatory and conspecific fear and for the reaction to pain (Silva, Gross, and Gräff 2016), which usually result in an immediate reaction to the threat. More proposed categories additional to the already mentioned ones describe social, homeostatic (including pain-avoidance) and also existential fear (LeDoux and Brown 2017), which are usually not associated with an immediate physical response.

To simulate a natural threat perception moment, it is necessary to generate an ambiguous and innately threatening moment.

2.3.1 Predatory fear

is associated with carnivorous animals. It requires an immediate response and is highly relevant to survival. The pathways of predatory fear are context and stimulus dependent and involve separate nuclei of the amygdala. For example, if the stimulus is olfactory, then the accessory olfactory system (or bulb in the case of rodents) signals predator cues to the medial amygdala, which will project to the hypothalamus (Silva, Gross, and Gräff 2016). The main olfactory system will also signal to the cortical amygdala, but how the outputs of this section influence the defensive response is unclear. This same predator integration circuit also receives information from multimodal (auditory and visual) stimuli in the cortex, via the basolateral and basomedial amygdala (**Figure 4**). The integration circuit in the hypothalamus consists of anterior hypothalamic nucleus, the ventromedial hypothalamic nucleus and the dorsal premammillary nucleus. One key output of hypothalamus is to the dorsal periaqueductal gray, which mediates the defensive responses (Gross and Canteras 2012; Silva, Gross, and Gräff 2016).

Most of the response following predatory fear is based on context and external influences, like the proximity, position, and type of predator. If escape is possible, then it is the dominant response. The speed and path of flight depends on the distance of the subject from the predator. If contact between subject and predator occurs, then the subject can take defensive measures (e.g. vocalize) or attack the predator. If escape is impossible, subjects can try to avoid detection, by freezing or by facing the predator. This behavior continues, until the defensive distance is reduced to nearly contact, whereupon it will be again replaced by attacks and vocalization (Blanchard and Blanchard 1989).

Olfactory: Olfaction is a key sense in rodents, and mice respond to olfactory threat cues. There are some olfactory cues which drive innate defensive responses (Stowers and Kuo 2015). These innately threatening odorants include secretions by predators, such as excrements or saliva (Isogai et al. 2011), or even pheromones secreted by stressed conspecifics (Stowers and Logan 2010).

This property of murine defensive behavior has been utilized in predator fear conditioning, which follows the same pattern as fear conditioning involving foot shocks, just with an predator-associated odorant rather than an aversive and painful foot shock (Takahashi, Chan, and Pilar 2008).

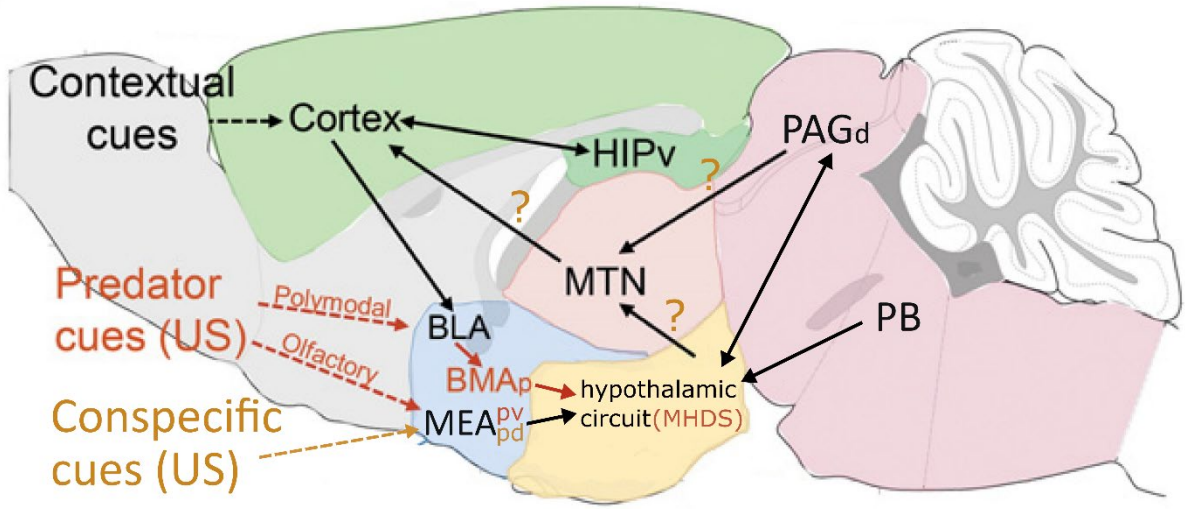

Figure 4 *Comparison of the pathways proposed for generating memories of predatory and conspecific fear.*
Memories of innate fear involve neurons distributed in the amygdala, hippocampus, and cortex (black lines). Predators are identified by polymodal and olfactory stimuli, which are processed in distinct locations in the amygdala and transferred to the medial hypothalamic defensive system (MHDS). The MHDS also receives projections from the parabrachial nucleus (PB), which is thought to convey pain signals during the encounter with the predator. After the sensory information has been integrated in the MHDS, downstream connections via the periaqueductal gray (PAGd) and directly to the midline thalamic nuclei (MTN) project into cortical regions involved in contextual fear learning. The connections listed here for memory of conspecific fear are mostly theoretical. The circuits have not yet been fully investigated. But it is thought that cues regarding aggressive conspecifics trigger activity in amygdala which modulates the MHDS hypothalamic circuit. The hypothalamic link to the PAGd and MTN are also thought to play a role. The Parabrachial nuclei provide nociceptive signals to the hypothalamic nuclei that might emerge during attacks by the aggressive conspecific. The connections from the MTN and cortex are then then thought to trigger or consolidate memory formation.
Legend: green – cortex; blue – amygdala; yellow – hypothalamus; pink – brainstem.
Figure 2A, B, adapted from: Silva, Gross, and Gräff 2016.

Visual: Prey-animals have an innate fear of "looming" predators. This behavior is critical in environments where little cover is available and thus fast reaction to an approaching stimulus is required to survive. The reflex, guided by vision, to "duck" away from a rapidly approaching object exists in adult and infant rhesus monkeys and in other species including human beings (W. Schiff 1965). A key requirement for a response is that the stimulus is darker than its background and rapidly increases in the field of view, where the rate of magnification correlates to more abrupt responses. Another detail to this response is that some species are capable of interpolating a "path" of the virtual object from the shown stimulus and react accordingly to a skewed magnification (W. Schiff 1965). The same behavior has also been observed in mice, where it was shown to be an essential reflex, presumably required to avoid aerial predators. Since it can be observed on the first exposure to the stimulus, and is as reliable as other vision-based reflexes, it has been suggested that the looming response in mice also originates in a dedicated retinal module, probably in the form of one of the retinal cells with a transient OFF-channel, projecting into the superior colliculus (Yilmaz and Meister 2013).

Auditory: This behavior is not restricted to visual stimuli and can also be elicited by complex auditory cues (Ghazanfar, Neuhoff, and Logothetis 2002).

Another approach to induce innate fear has been to present the lifeless body of a predator. This approach has been used to research the defensive responses in the immediate confrontation of a mouse with a (terminally sedated) rat (Blanchard et al. 1998). With this approach, it has been possible to observe differences in the behavior of laboratory mice compared to wild-type mice. The differences relate to domestication-linked changes in defense, caused by human selection of mice with a reduced display of defensive threat (Blanchard et al. 1998).

While rats show predatory behavior to a wide range of species, the predatory behavior to mice is not ensured to occur. Eighty percent of rats do not show aggression towards mice and even during starvation will not become aggressive, leading to them starving to death. In the 20% of rats where this behavior occurs, it is highly stereotyped, with the attack always concluding in multiple bites in the cervical spine of the mouse, thus killing it (Karli 1956). This predatory behavior can also be induced in the non-killing rats by electrical stimulation (Panksepp 1971) and can be modified by cholinergic stimulation of the lateral hypothalamus (Smith, King, and Hoebel 1970). Twenty percent of the rats, which show no aggression to mice, show carrying behavior near mice, although this behavior is dynamic and may transfer to a killing behavior. This is theorized to be either an incomplete killing response, since the carrying behavior mirrors the killing behavior, except for the lethal bite, or a response distinct from aggression and originating in parental behaviors towards rat pups (Lonowski, Levitt, and Larson 1973).

2.3.2 Conspecific fear

occurs when faced with aggressive conspecific. This type of fear is not as well researched as predatory fear, but circuits relating to olfactory conspecific stimuli have been identified. The related circuit resembles the olfactory predator circuit but shows differences in which section of the hypothalamus and amygdala are involved and has no overlap with the ones related to the predatory integration circuit (Silva, Gross, and Gräff 2016). After the olfactory signal has been transferred from the accessory olfactory system, it is transferred to the posterior dorsal medial amygdala and from there to the hypothalamic integration circuit associated with conspecific fear. This consists of the medial preoptic nucleus, the ventrolateral section of the ventromedial hypothalamic nucleus, the ventral premammillary nucleus and the dorsomedial section of the dorsal premammillary nucleus. It then, just as the predatory integration circuit, projects to the dorsal periaqueductal gray (Silva, Gross, and Gräff 2016).

Just like the pathways involved in conspecific fear, the resulting responses are not currently researched in-depth and still have many open questions. Nonetheless, current research shows an overlap between neuron populations involved in the medial hypothalamic circuit during social aggression as well as sexual and maternal behaviors (Gross and Canteras 2012) and that during early stages of mating behavior and aggression overlapping subpopulations are involved, which are inhibited as mating progressed.

2.3.3 Homeostatic fear

can be described as the fear of noxious stimuli, and conditions. Fear responses to pure noxious stimuli are not sufficiently researched to know whether these stimuli are in fact able to induce an innate fear response on their own (Silva, Gross, and Gräff 2016). Pain is one widely studied noxious stimulus. Its emotional processing is mostly associated with learning, and the associated circuits are found in the basolateral amygdala complex. Although it is commonly assumed to also cause innate fear, Silva, Gross, and Gräff state in their 2016 paper that pain might be considered as a signal of harm that has already occurred, and supports fear learning, rather than being the inducer of fear itself.

There are also other noxious situations, which initiate an emotional response, in the form of suffocation and hunger. There are other situations, for example the emotional response to drowning or heat exposure, that are not well studied at all (Betley et al. 2013). A proposed circuit for starvation and hunger by Betley et al. from 2013 contains parallel and redundant features, which originate in distinct subpopulations of agouti-related protein-expressing neurons in the hypothalamic arcuate nucleus and project to locations in the forebrain.

2.3.4 Social fear

occurs in connection with social stress, social isolation, social instability, and social defeat. It is thought to be one of the most common symptoms of social anxiety disorder in humans. In mice it can be experimentally induced by conditioned defeat, maternal separation or chronic subordinate housing (Toth and Neumann 2013). Recent research has shown that a locus in the ventromedial thalamus previously only associated with sexuality and aggression was also involved in social aggression and social fear, in the form of a largely (~80-90%) non-overlapping neuron population. The small overlap between the populations is thought to be related to fear induced aggression (Sakurai et al. 2016).

Research into the role of neurons in the prefrontal cortex in social fear expression was originally based on findings that prefrontal hyperactivity is a cause of hyper-responsive threat processing (Kawashima et al. 2016). These studies showed that there exists a local circuit of parvalbumin interneurons that inhibit pyramidal neurons' firing and in turn are themselves inhibited by somatostatin interneurons, leading to a disinhibition of prefrontal pyramidal neurons by somatostatin inter-neuronal activity, which cause a display of social fear responses (Xu et al. 2019).

Responses to social fear include reduced interaction with conspecifics, including a slowed speed during approaches, and a change in posture, i.e. a stretched posture (Xu et al. 2019). In humans, social fear represents one of the main symptoms of social anxiety disorder, which is the second most prevalent anxiety disorder, after generalized anxiety disorder and followed by posttraumatic stress disorder. It is generally identified in two main forms: a specific form, which includes the fear of public speaking, and a generalized form, which is characterized by the avoidance of all social situations. This disorder has been described as a potential major risk factor of other affective disorders, like major depressive disorder or Prader-Willi-syndrome, due to it being highly comorbid with these and often emerging first (Neumann and Slattery 2016).

2.3.5 Existential fear

is commonly assumed to only exist in humans, since fear based on the finite nature of existence requires an awareness of existence, and time. According to the available literature, this has not yet been observed in any species beside Homo sapiens. Even in humans this type of fear is commonly spoken about in only its psychological aspect in connection with individual plans for life in the face of death (Neimeyer and Chapman 1981) or in the context of end-of-life palliative care for, for example, patients with advanced cancer (Breitbart 2017). Likely due to its complex nature, there do not seem to exist any proposed circuits or loci associated with this type of fear in the available literature.

Responses to existential fear are, just as its underlying neural circuits and correlates, not deeply researched. Most known is the existential crisis, which originates in the awareness of one's own approaching death and the inability to reconcile this fact with a personal perspective on the meaning of life (Yang, Staps, and Hijmans 2010). This response is highly individual in its nature and usually researched in a psychological context, with less focus on statistical approaches rather than individual case studies (for example Renz et al. 2018).

2.4 Learned fear is, next to innate fear, the other overarching type of fear. It will not be applicable in the simulation of an innate threat perception moment but is one of the most common methods to elicit fear. It relies on the association of an unconditioned, innately fearful stimulus with another originally neutral stimulus. Innate threats, for example the presence of a predator, leads to defensive behavior, since animals are naturally selected to protect themselves from harm associated with that threat, in this case being devoured by the predator. Yet the same behavior can be elicited by cues, which were previously associated with the exposure to a predator (**Figure 5**). This phenomenon is called fear conditioning (Gross and Canteras 2012).

2.4.1 Fear conditioning has been used since at least the 1940s (Mowrer and Lamoreaux 1946). It has been used to understand the processes behind learning and threat avoidance. One of the first paradigms used noxious foot shocks to explore the neural circuits involved in the processing of pain, and to determine whether an intervention via electrostimulation extinguished the innate fearful reaction to pain (Cox and Valenstein 1965). These experiments show that the fearful response depends on the internal processing of the painful stimulus.

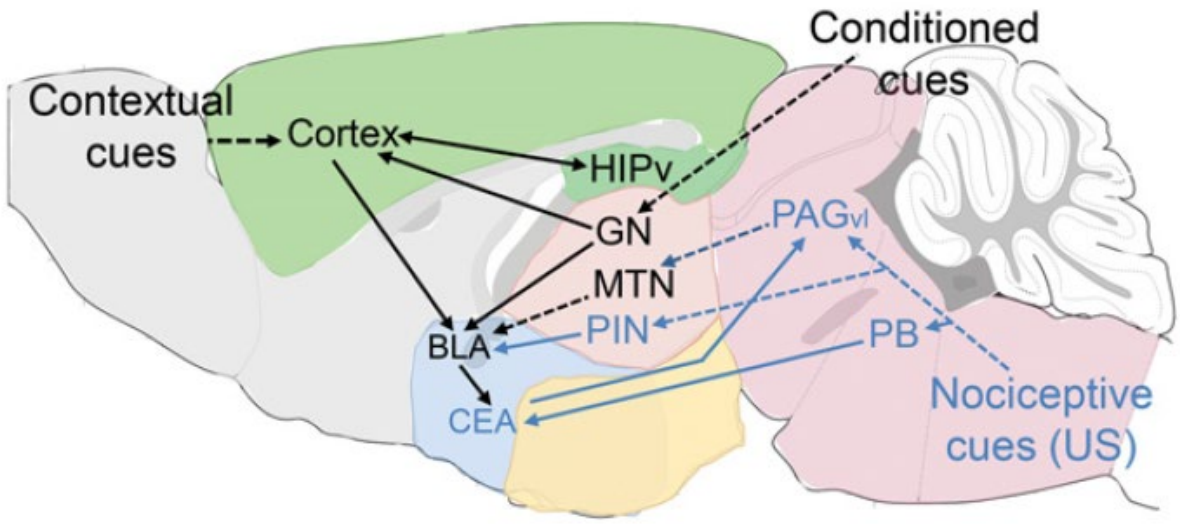

Figure 5 *Circuits proposed for remembering a conditioned fear stimulus.*
Contextual cues are transmitted to the basolateral amygdalar complex (BLA) by the cortex and ventral hippocampus via cortico-thalamic inputs. Conditioned cues, for example auditory signals, are transferred to the BLA and cortex by sensory nuclei in the thalamus, such as the geniculate nuclei (GN). It is not yet definitely known how nociceptive cues reach shared fear memorization system. Proposed pathways involve spino-thalamic projections via the posterior intralaminar thalamic nuclei (PIN), input from the ventrolateral periaqueductal grey (PGAvl) to the BLA through the MTN, and a direct connection from the PB to the central amygdala (CEA), which would in turn mediate defensive behaviors through projections to the PGAvl.
Adapted from: Silva, Gross, and Gräff 2016, Figure 2C

3. Design process

Here I will describe our rationale and thinking process for designing a novel behavioral paradigm that incorporates ambiguity and fear. Our primary requirement was to elicit innate fear in mice, and to make the threat perception moment ambiguous by making it multimodal and titratable for distinct sensory stimuli. This, in turn, led to the design choice of a rat as the innate stimulus. Over time, mice could learn to associate particular conditions of the rat stimulus, and this might be a conditioned stimulus, but there is no explicit use of conditioned stimuli in our paradigm. Threat assessment with a conditioned stimulus would occur in a different manner, by using a memory associated with the CS.

Because our approach and design are novel, there is no existing apparatus to induce a natural rat related predatory threat in mice. Therefore, we created a new apparatus that included many new design elements (ambiguity, changing the sensory stimulus, etc.). It was also somewhat incumbent on us to avoid using traditional methods for eliciting fear. We would not use foot shocks, air puffs, or looming stimuli.

The use of an animal that could be a predator, and that was available in a laboratory setting had an additional benefit. A rat could be presented in a controlled fashion to mice, where the mice could be allowed to only see, smell, or hear the rat, or could have multimodal almost tactile interaction with it. Under these circumstances, the moment a threat is perceived could be tracked behaviorally and by recording from the brain, while we could at the same time control the sensory aspects of the threat. To allow the observation of the neural mechanisms involved in threat assessment, this setup had to be able to generate and measure the **four Fs** of fear: *flight*, *freezing*, *foraging,* or *fighting*. To reduce harm to the animals, we avoid the fourth element, fight. Mice had to be able to run away from the threat, continue eating as if there was no threat, or freeze from fear.

One of the first options that we considered in the design process was to use a floating platform, the Air-Track (Nashaat et al. 2016) that was designed and built in-house in the Larkum laboratory. The Air-Track allows mice to move a platform that floats on air, despite the mice being head-fixed. Our design would have involved linking the movement and rotation of the platform, to the presentation of a threatening stimulus, the rat (**Figure 6**).

We considered incorporating a rotating cube that had four faces with distinct structures, which would allow for four different stimulus presentations. This cube would have contained the live rat and would have rotated along with the movement of the platform. The design would have involved a discontinuous stimulus condition and required more design elements to allow the reward spout to potentially rotate with the rat in the tube. However, to avoid problems with the position and presentation of the rat in the cube, we decided to replace the rotating cube with a static tube, and changed the stimulus parameters by moving a disk around the mouth of the tube. The disk would have had four sectors for the four stimulus conditions.

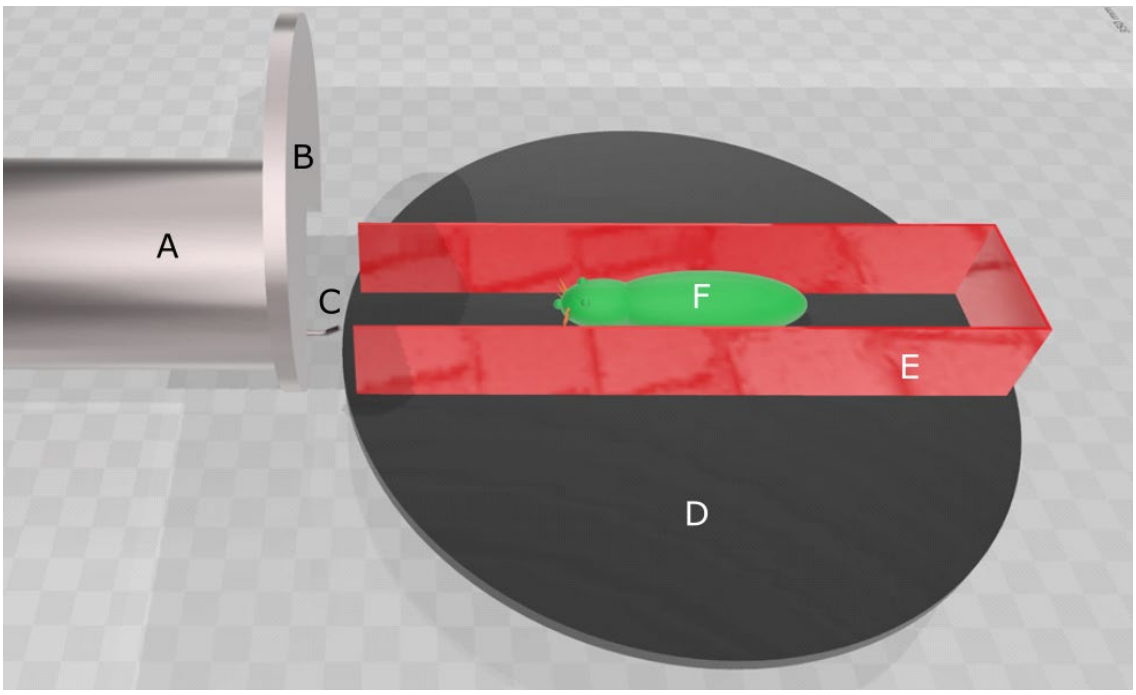

Figure 6 *Early three-dimensional model of the setup depicting a previous version utilizing an Air-Track-system.*
A) Tube containing a live rat. Moves in sync with the outer edge of the Air-Track platform **D**. **B**) Rotating disk masking part of the rat stimulus. Has multiple sectors. Sectors not shown here. **C**) Licking spout. Dispenses water if approached and licked. **D**) Floating Air-Track platform. Moves under the mouse, which is head fixed. **E**) Corridor made of opaque plastic. Guides the mouse along a one-dimensional path to the tube. **F**) Head fixed mouse

In this version of our design (**Figure 6**), the mice would have moved along a linear corridor, mounted on a floating Air-Track platform, and approached the tube containing the rat. They would have been trained to obtain reward from a licking spout at the bottom of the tube. The tube would move along a linear path in sync with the edge of the platform and thus the end of the corridor. Once the mouse received its water reward, the tube containing the rat would move back to its starting position and the mouse would have to reset the setup for the next trial by turning the platform around and returning to the starting position at the other end of the corridor. At this position, the mouse would have to face the tube before the next trial would begin.

However, this approach introduced an additional unnecessary behavior, the rotation of the platform by mice, to the paradigm. Since the movement expected of the mouse was one-dimensional (forward or backward) to begin with, there was no reason to continue the design with a two-dimensional Air-Track platform. Due to this we decided to move to a treadmill (Poort et al. 2015) instead, where the back and forth movement of the rat in a tube was linked to the movement of the treadmill (**Figure 7**). An additional advantage over the Air-Track was that the mouse could now face the stimulus, the ambiguous threat, without any interruptions by the walls of the platform.

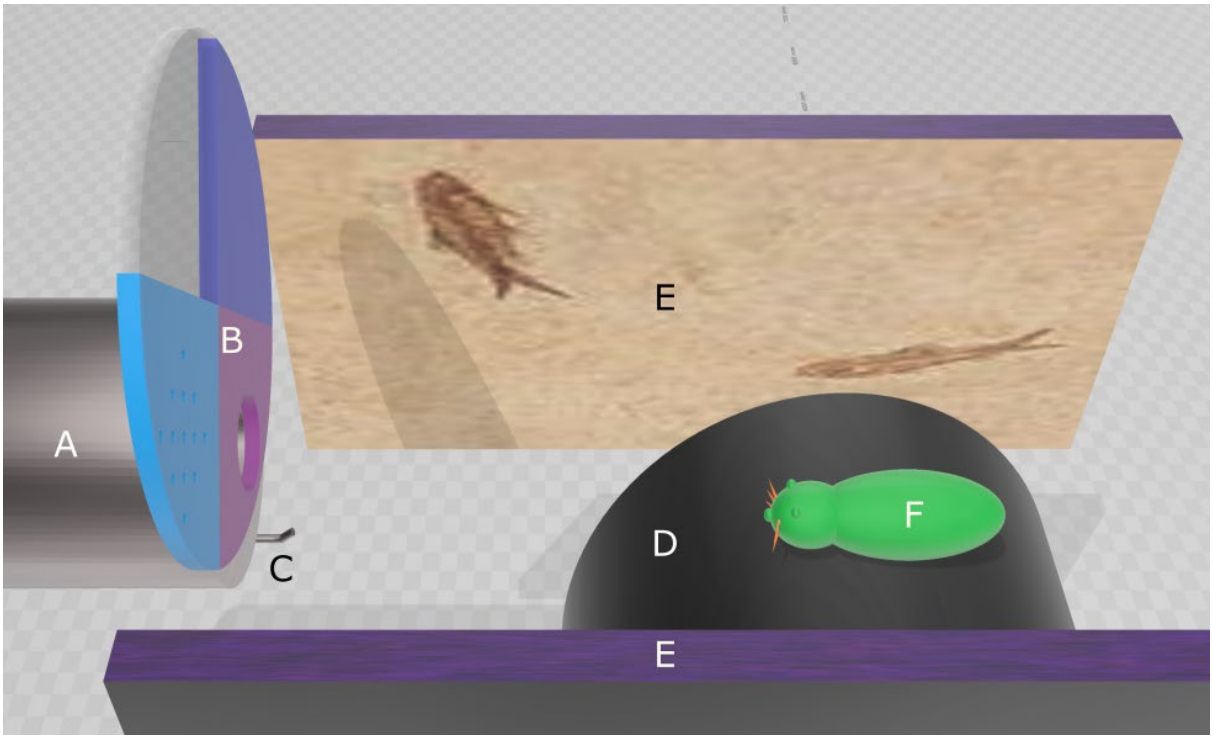

Figure 7 *Initial three-dimensional model of the final version of the setup: Air-Track platform replaced with a treadmill.* ***A****) Tube containing a live rat. Moves in sync with the rotation of the treadmill* ***D****.* ***B****) Rotating disk masking part of the rat stimulus. Has multiple sectors.* ***C****) Licking spout. Dispenses water if the tube has reached the mouse and the mouse has licked.* ***D****) Treadmill which is moved by the mouse and translates it rotation into an analog signal.* ***E****) Virtual movement context on two widescreens, which are positioned along the sides of the setup.* ***F****) Head fixed mouse*

Each trial would now consist of a simple approach towards the tube, with the reward dispensed once the mouse had reached the tube and licked the waterspout. If the trial timed out or the mouse obtained a reward, the tube would move back to its original position. Although this solved the problem of the setup reset for the next trial, it also meant that the mouse lost important movement context when the linear corridor with walls was replaced with an open treadmill. To replace this lost movement context, two screens were added which showed a synchronized moving pattern to simulate a virtual corridor.

Once the decisions about the general layout of the setup had been made, there was only the question of the mechanical propulsion that remained, which would drive the tube and rotate the disk. A silent chain, driven by a stepper motor, was selected from a range of mechanical actuators to move the tube back and forth. A motor of the same type was also used to rotate the stimulus modulation disk, which simplified control of the setup.

4. Methods

4.1 The materials that we used in the construction of the setup will be described in detail here. These consist of mechanical and digital elements required to simulate the virtual movement of the mouse towards the tube, and the behavior equipment to gain detailed information about the behavior and state of the mouse and rat during the experiment. Below, I will describe each of the functional elements in the setup beginning with the mechanical components, followed by the digital control elements and the recording equipment.

4.1.1 The mechanical components of the apparatus consist of a treadmill, a tube for holding a rat, a disk, and a reward spout. The treadmill (Marker A in **Figure 8)** is circular. It is made from rigid foamed plastic that has rubberized outer coating. It is lightweight enough for a head-fixed mouse to move it, while maintaining a sufficient level of grip and footing. The red acrylic tube (30 cm long, 7 cm in diameter) that houses the rat (Marker B in **Figure 8**) is intended to generate innate fear in the mouse. Mice must choose between obtaining a reward from the spout just below the tube that contains the rat (Marker E in **Figure 8**) and a fearful reaction to the rat stimulus. The red color is meant to reduce the possibility of unintended visual interaction between rats and mice.

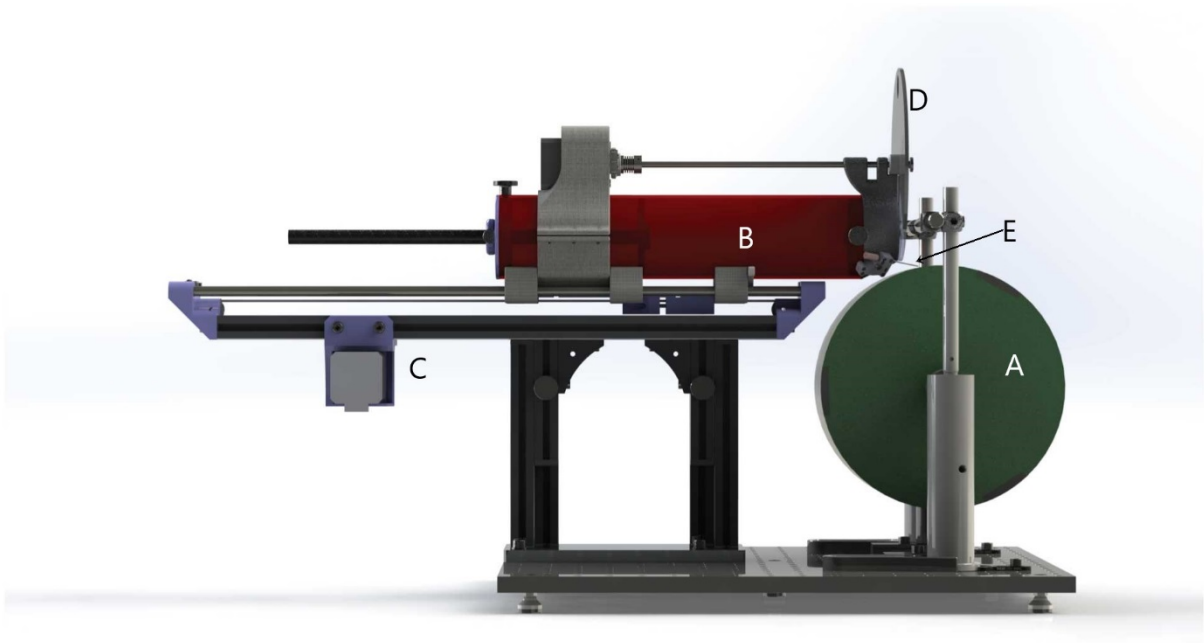

Figure 8 *Overview of the mechanical components in the setup.*
A*) Treadmill that mice walk on.* ***B****) Tube that holds a rat.* ***C****) Stepper-motor, which drives the movement of the tube along the rail.* ***D****) Disk divided into 4 sectors corresponding to 4 distinct stimulus-conditions.* ***E****) Licking spout, used to dispense a reward once the mouse has moved far enough*

A manually controlled piston is used to position and nudge the rat in relation to the opening facing the mouse (**Figure 8**). Odors can be actively removed from the tube by creating an airflow towards the back end of the tube with the help of a TTL controlled vacuum-line. When a pinch valve controlling the vacuum-line is activated, odors are no longer removed.

The tube is positioned atop a rail (Marker C in **Figure 8**), which is linked to a stepper motor that controls the position of the tube. The output of the treadmill is processed and translated into a pulse-width modulated signal, and this output is used to calculate the extent and direction of movement to impose on the tube. The rail that the tube moves on has small trigger switches. Contact with these switches occurs at the two most extreme positions of the rat tube, which are used as reference points to calibrate the position of the tube on the rail.

The stimulus modulation disk (Marker D in **Figure 8**) is mounted in front of the tube on a rotating axle, which is connected to a second stepper motor. It allows four different stimulus conditions: auditory, auditory-visual, auditory-olfactory, and auditory-tactile. The auditory stimulus is always present, since the removal of ultrasonic vocalizations in a moving and lightweight setup is not easily possible, and it will thus be used as a baseline throughout the different modulations. At the beginning of each trial one of the four sectors of the disk will be rotated over the opening of the tube and thus control which stimulus modulation will be active during the trial.

The licking spout (Marker E in **Figure 8**) is used to reward the mouse with a small amount of water whenever it approaches the tube completely and licks the spout. Mice are first trained to move the treadmill to bring in the reward spout. In the first sessions, no rat is used in the tube. The goal is simply to train the mouse to be aware of the lick tube movement and location, and to habituate mice to the moment of the reward delivery.

4.1.2 The digital components are those that measure, monitor, and calculate the movements of the setup in reaction to the movement of the mouse. These parts include a Bpod r2, a Raspberry Pi 4, and an Arduino (shown in **Figure 10** and **Figure 11**) Any movement of the treadmill is transmitted to an electrical circuit mounted on its axle, which translates the rotation to two analog signals correlated to angle and velocity, with a voltage between zero and five volts. The angle-encoding signal will be processed by the digital components to detect the virtual position of the mouse and let the virtual environment and the tube react in real-time to its movement.

A Bpod by Sanworks LLC is used to control timing and states during the trials. This device is based on a Teensy 3.6 USB development board and is specialized for the automatic control of behavioral experiments by using four ports to control LEDs and solenoid valves, and record signals from light-gates. Two BNC-inputs and two -outputs serve as an interface for TTL-pulses and allow the Bpod to receive accurate signals from external equipment, such as triggers for state-transitions, or send TTL-pulses to other components, such as the triggers for the individual frames recorded by the cameras. It also allows for the accurate control of reward amounts from solenoid valves by calculating the opening time from a calibration curve.

The Raspberry Pi 4 is the currently newest version of a series of single-board computers developed by the Raspberry Pi Foundation. It possesses a quad-core processor and an operating system with a graphical user interface, which allows it to take care of drawing the movement context on two wide screens and controlling the movement of the tube at the same time.

An Arduino Nano was utilized to offload some of the processing power required to control the stepper motors in the setup from the Raspberry Pi. It is a small, complete board based on the ATmega328 microcontroller. The Raspberry Pi transmits a signal, which instructs the Arduino on where to move the disk and tube.

4.1.3 Recording components record movement and vocalization of the mouse and rat, and the facial expression and whisker movement of the mouse throughout the experiment. These components are cameras and ultrasonic microphones.

On the next page:
Figure 9 *Connections between elements of the setup.*
Diagram showing the connections in the setup. A top-down view of the mechanical components of the setup is shown on the right side, the control elements are shown on the left side. Input to the mechanical elements (green), output to the control elements (red), and communication between two elements (blue) is shown in the diagram.

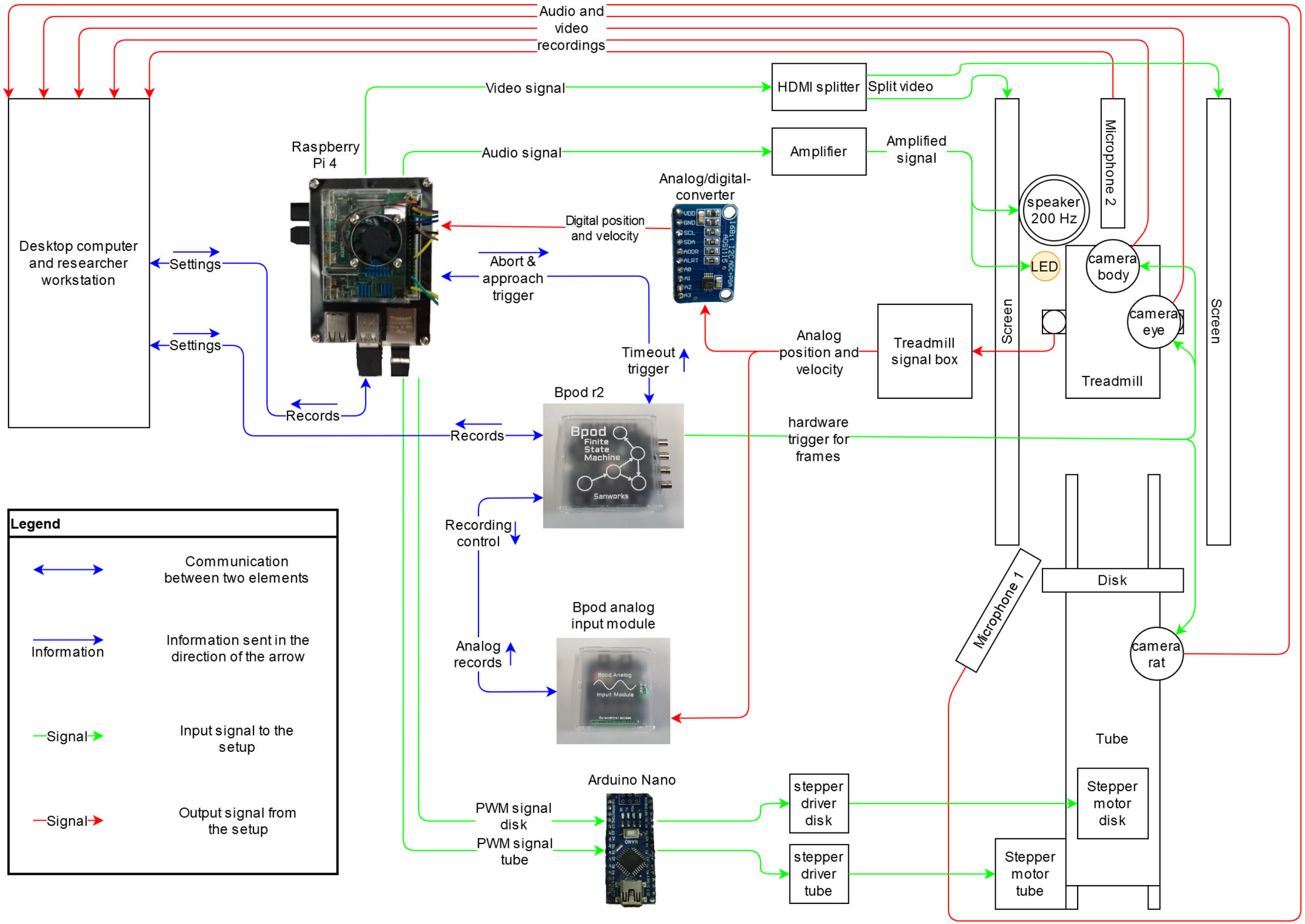
Audio and video recordings
Desktop computer and researcher workstation
Settings
Settings
Raspberry Pi 4
Video signal
HDMI splitter
Split video
Audio signal
Amplifier
Amplified signal
Analog/digital-converter
Digital position and velocity
Abort & approach trigger
Timeout trigger
Records
Records
Bpod r2
Bpod
Finite State Machine
Sanworks
Recording control
Analog records
Bpod analog input module
Bpod Analog
Input Module
Analog position and velocity
Treadmill signal box
hardware trigger for frames
speaker 200 Hz
LED
Microphone 2
camera body
camera eye
Treadmill
Screen
Screen
Microphone 1
Disk
camera rat
Tube
Stepper motor disk
Stepper motor tube
Arduino Nano
PWM signal disk
PWM signal tube
stepper driver disk
stepper driver tube
Legend
Communication between two elements
Information
Information sent in the direction of the arrow
Signal
Input signal to the setup
Signal
Output signal from the setup

A desktop computer will control all the settings used during the experiment and will record the input from three cameras and two ultrasonic microphones. During the trials, the computer will serve as a controller with which the researcher can supervise the experiment with the help of the camera feeds, a real-time trace of the movement of the treadmill and the vocalizations of the mouse, and a statistical analysis. The computer also handles initialization and shutdown of the whole setup. The cameras used in this experimental setup are made by Basler AG. One of the cameras records the full body position of the mouse, along with a smaller region that records the whisker movement. This smaller region is recorded at two hundred frames per second, while the larger (full body) works at one hundred frames per second, which is the same frequency as the other cameras. To record the pupil movement and dilation an infrared sensitive camera is used. This camera is mounted next to the full body/whisker camera and will be redirected by a small mirror mounted to the side of the mouse. The third camera is mounted facing the tube containing the rat and record the rat's position and behavior during the trials.

Two microphones are part of the setup and are used to record the vocalizations of the mouse and rat. To be able to determine the location of the emitted ultrasonic sounds, one of the microphones is mounted behind the mouse, which will allow a recording of the sounds as the mouse would hear them, and the other one at an angle below and beside the rail carrying the tube, which will mostly record sounds emitted by the mouse.

To synchronize the cameras with the microphones, a low frequency sound of about two hundred hertz will be emitted by using the 3,5-millimeter audio jack on the Raspberry Pi 4 to transmit a signal to an audio amplifier, whose output will then drive a full-range speaker and a LED at the same time. By aligning the first frame captured by the full body camera showing the active LED with the first microphone sample, which shows the low frequency signal, a high level of synchronization between both devices can be achieved.

4.1.4 Two widescreens

mounted to both sides of the treadmill will provide movement context to the mouse. The pattern shown on them is random and mirrored along the horizontal axis, to allow the generation of a single screen, which is then split and drawn to the second screen, which is turned upside down. This enables the context to be drawn and moved with the treadmill with little delay, since nearly half of the processing time for two screens can be avoided.

The random pattern consists of a collection of markers, from which one is randomly drawn whenever the mouse moves far enough in a single direction. This distance is determined by the buffer size, which is assigned before the experiment starts and defines the number of markers that are remembered when they leave the screens' edge. Due to this, there is a level of persistence in the shown pattern, which will relay a movement context that is more natural than a completely random one.

4.2 The code and implementation

had one objective, that the components that moved -- the input from the treadmill, the output to the tube and visual context were synchronized to a level which would feel natural to the mouse in the setup. For that purpose, all these elements are controlled with the same Raspberry Pi 4, to prevent any delay, which could be introduced by inter-element communications or additional processing of cameras or microphones on the same platform. The remaining functions, controlling the flow of the trials and recording the behavior of the mouse and rat, were moved to a Bpod finite state machine and a desktop computer.

4.2.1 The Raspberry Pi 4

is used to read the analogue movement signal from the treadmill as input, which is then processed and converted into a digital signal (**Figure 10A**). The movement of the treadmill is read-in by translating the output from the treadmill's two analog traces that run from 0-5 volts to a signal, which can be read by the Raspberry Pi. To achieve this, an ADS1115 analog to digital converter from Adafruit Industries is used (**Figure 10C**). This chip transmits the digital signal to the Raspberry Pi via an I2C (inter-integrated circuit) serial communication bus. Since both output channels, one for the position and one for the current speed, are redundant in their information, the internal representation is computed from one of them, the position, while both are recorded.

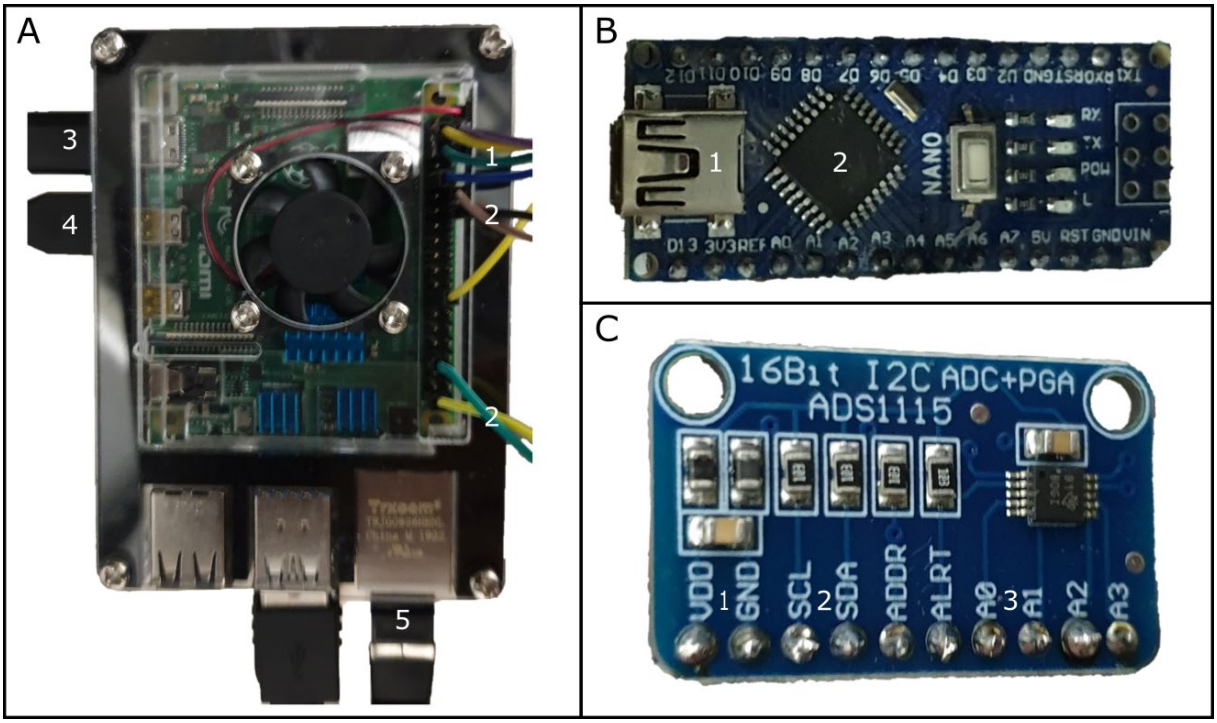

Figure 10 *Hardware control elements.*
A*) Raspberry Pi* ***1****) I2C-connection and power supply to analog-digital-converter (ADS1115).* ***2****) PWM-connections controlling the tube and disk, to Arduino.* ***3****) 5V power supply.* ***4****) HDMI-output to screen.* ***5****) Ethernet-connection to desktop computer.* ***B****) Arduino Nano* ***1****) 12V power supply.* ***2****) Processor.* ***C****) ADS1115.* ***1****) 5V power supply from Raspberry Pi.* ***2****) I2C-communication from Raspberry Pi.* ***3****) A0 and A1 channels used to receive analog signal from treadmill.*

To process the movement signal it is necessary to know the diameter of the treadmill, the distance of the tube and the pixel-density of the screens. This information can be used to translate the analog voltage-encoded position to the same real-world length on all three devices. For this step, the treadmill diameter is measured in centimeters and translated into its corresponding circumference, which is then used to calculate the volt/centimeter travelled. The result is multiplied with a pre-determined factor, which can be reset to change the speed with which the tube and the visual context move.

This aspect of the design is intended to allow for adjustments to the speed, changing the effect of the mouse's movement on the treadmill on the position of the reward spout and rat. We expect to use this feature during the habituation phase and during the learning phase where mice learn the behavioral task. Mice can be given reward faster or slower for smaller or larger movements of the treadmill. During active trials with a live rat, it is possible to modify the movement of the tube in relation to the fear displayed by the mouse on each trial.

The tube and the screen are both moved by the real-world distance calculated according to the output signal of the treadmill. The screens are drawn directly on the Raspberry Pi with the help of the Python library Pygame, which was originally written for the use in the development of video games. To move the tube, the Raspberry Pi translates the target location into a relative value encoded in a pulse-width modulated (PWM) signal.

4.2.2 The Arduino Nano

(**Figure 10B**) takes the PWM-signal from the Raspberry Pi and uses this to instruct the stepper motors to move the tube to the target position. This is done to avoid having to use the Raspberry Pi to control the stepper motors, which require continuously updated commands and thus add delay in the processing of movement and the control of the other elements.

To control the position of the rotating disk at the front of the tube and the modulation of the fearful stimulus, the Arduino receives a secondary PWM-signal on a separate channel, which describes the currently selected mode. This signal originates in the desktop computer at the beginning of each trial and is sent to the Raspberry Pi before being translated into a PWM-signal for the Arduino.

4.2.3 The Bpod r2 finite state machine (**Figure 11A**) is used to synchronize the processes and stages in the active trials. It receives a preprocessed state matrix, which includes information about the length and the potential triggers during each trial state, and then proceeds to measure the timestamps of inputs and the time spent in each state. Once the tube has reached the closest position to the mouse, the Raspberry Pi sends a trigger to the Bpod, which activates a reward state. During this state, the mouse can lick at the waterspout, which is equipped with a light gate. The reward is then dispensed by the Bpod by way of opening a solenoid valve, which allows the flow of the water through the spout. If the mouse decides to flee during this state, the tube is moved to the farthest position and the trial is aborted. A signal is sent out to a Bpod, which then triggers the trial abort state in the state machine.

The Bpod is also utilized to synchronize the recorded frames from the cameras. It uses a global timer as a hardware trigger for every single frame. This minimizes the delay between the frames acquisition in each video stream. An additional component, the analog input module (**Figure 11B**), records the analog position- and speed-trace of the treadmill.

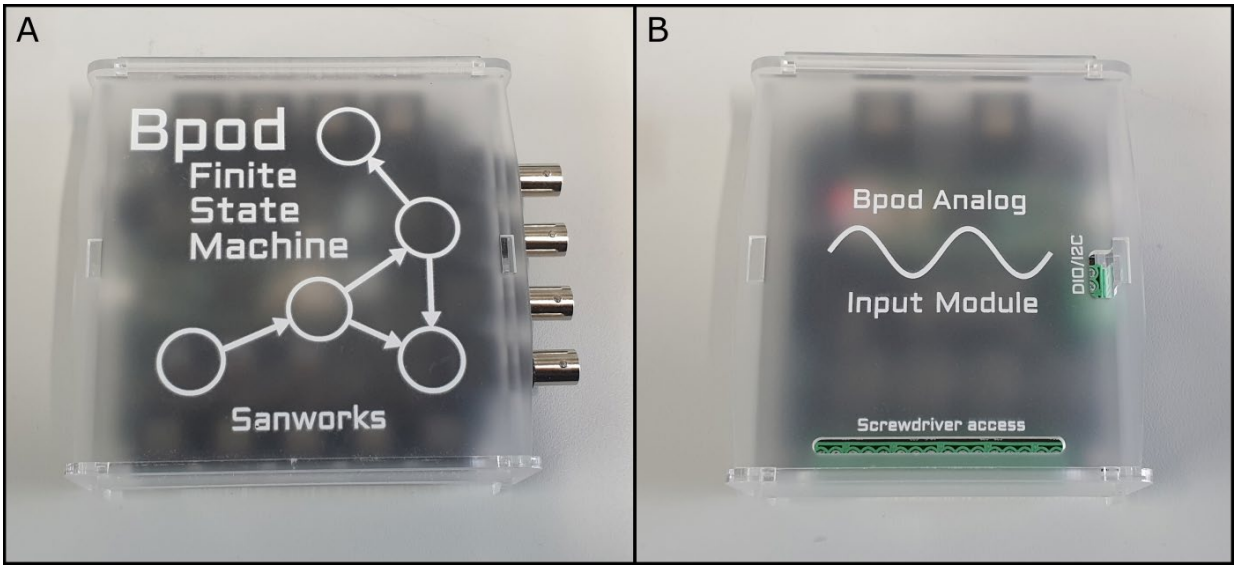

Figure 11 *Trial control elements.*
A) The Bpod finite state machine is used to control timing and sequence of trial stages and detects signals from the Raspberry Pi to determine stage transitions. It also communicates beginning and end of each trial to the desktop computer and Raspberry Pi and controls the dispensing of reward. During the trial, it records accurate timestamps for every received and transmitted event. **B**) The Bpod analog input module records an analog trace of the treadmill signal with a high sampling rate (up to 10 kHz). It is controlled by the state machine and transmits a copy of the high-resolution trace to the desktop computer after the end of the trial.

4.2.4 The desktop computer

runs the software which generates the interface and feeds the input parameters to the other components. It also uses the pypylon software interface for the Basler cameras in the setup and uses the PyAudio library to control the input from the two microphones.

The interface was programmed to offer the researcher a high amount of information, while still maintaining a structured overview over the current state of the mouse and setup. During an active experiment, the researcher can see statistical information over past trials, movement trace and vocalizations in the current trial, a short statistical summary of the currently running trial, and the input from the three cameras.

To synchronize the recorded information, built-in functions are utilized, such as the hardware trigger for the cameras, as well as self-made solutions, for example the low frequency tone used to synchronize the video- and audio-recordings. To record the analog output of the treadmill, an eight-channel input module for the Bpod is used, which allows a precise timestamping of the mouse-movement. The records in the Raspberry Pi contain information on the timestamp of the analog input, which it also receives, and the timestamp and value of the resulting movement, which was transmitted to the tube and screens. When these two values are compared, an accurate delay between the movement by the mouse and its results shown in the position of the tube and the visual context can be determined. During the analysis of the recordings, this timeline can be aligned with the frames recorded by the camera, which were also triggered by the Bpod, followed by another alignment with the audio-recordings from the microphones, with the above-described method involving a low frequency sound and a LED. This procedure creates an accurately aligned dataset of multimodal recordings of the mouse, its behavior, and the resulting setup output throughout the entire trial.

4.3. The experimental protocol has two aspects: the trial protocol, which is described by the parameters and state matrix programmed into the Bpod, and the procedural protocol, which describes the manner in which the various aspects of behavior of the treadmill, tube and disk are controlled. Here we will describe both in the example of an experimental session.

4.3.1 At the beginning the researcher powers on the digital components of the setup. After booting, the Raspberry Pi automatically starts looking for a connection from the desktop computer, while the Bpod will be activated by it later. The desktop pc will start the interfacing module after it has finished the boot process, connects to the Raspberry Pi, and initializes the Bpod. After both components are active and connected, the software will start fetching frames from the cameras and microphones and display the camera feeds in the interface.

At this point, the researcher can activate the visual context and, if it is required, calibrate the end-position of the tube. The rat can be put into the tube, and the tube's back opening sealed again, before the mouse is introduced to the setup. After the visual context is activated and the rat present and hidden in the tube, the mouse can be head-fixed on the treadmill. Now the researcher can use the camera feeds in the interface to adjust camera position and angle, to get a clear image of the rat and mouse. A check on the visual context and output consoles of the Bpod and Raspberry Pi can confirm that the setup is active and ready for the experiment.

On the next page:
Figure 12 *Flowchart of the communications during the initialization, trials, and shutdown of an experiment.*
Upper flowchart, left side*. An experiment begins with the initialization of the components. The settings selected in the interface are transmitted to the elements, Bpod and Raspberry Pi, which then send a confirmation signal. After the Raspberry Pi has received the settings associated with the virtual movement context, it starts to display a virtual corridor, which is synchronized to the treadmill movement. This continues until the end of the experiment.*
Lower flowchart*. At the start of every trial, the Bpod state machine receives a state matrix, which it begins to run after it received the go-signal from the pc. From this point on, the desktop computer only receives signals, until the end of the current trial. The trial control is managed by the Bpod (timing and states) and the Raspberry Pi (treadmill position and fleeing). After the Bpod has sent its start-signal, which marks the beginning of recording, the Raspberry Pi activates the tube-movement and waits for the mouse to reach the tube. Should the mouse not reach the tube during the trial-state, then a timeout occurs and the trial ends. As soon as the mouse reaches the tube, the Raspberry Pi sends a trigger, which signals the Bpod to transfer to the reward state. In this state the Bpod waits for the mouse to lick the waterspout in a limited time window. Should this occur, then the reward is dispensed, and a short waiting period begins, else the trial times out and ends. During the entire reward period the Raspberry Pi can detect fleeing behavior (defined in the settings as a certain distance moved backwards) and can trigger a trial abort, which is signaled to the Bpod and causes the trial to immediately end. As soon as the trial ends, either by timeout or abort, the tube is moved to its original position away from the mouse and the desktop computer ceases any active recordings. Throughout the trial, the computer will record any triggers as markers in the video- and audio-recordings.*
Upper flowchart, right side*. After a trial-ending signal is received, the computer receives the records from the Bpod and Raspberry Pi and combines them with its own records from the cameras and microphones. Then a check occurs whether any more trials need to be run, which either results in the whole trial sequence being repeated with the sending of the state matrix to the Bpod or the experiment shutdown occurring. During the experiment shutdown the desktop computer sends a shutdown signal to both Bpod and Raspberry Pi and waits for any processes on the Raspberry Pi to cease. After this has been confirmed by the Raspberry Pi, any recordings can be optionally processed before the experiment ends and the researcher can begin another experiment at the setup.*

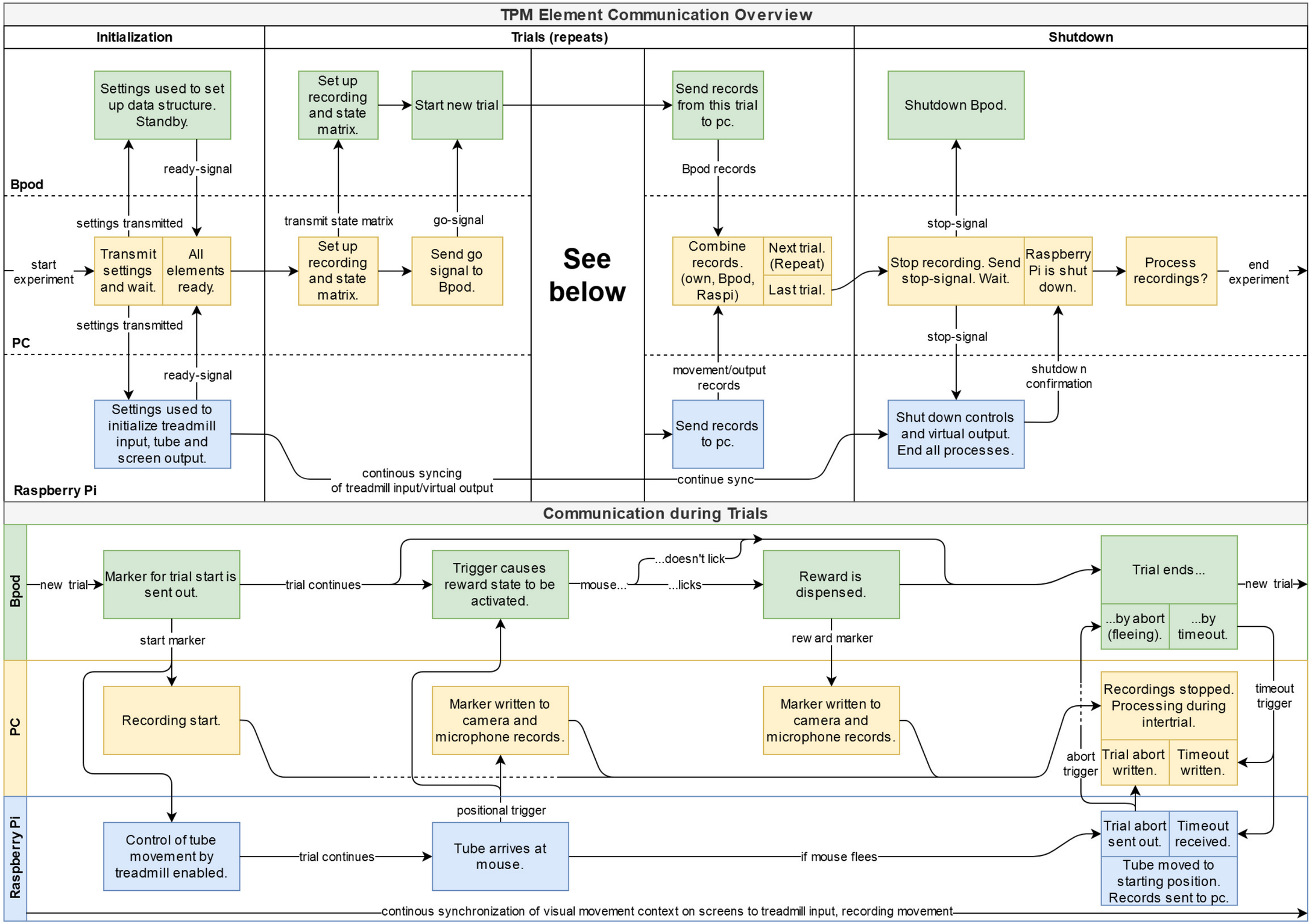
TPM Element Communication Overview
Initialization
Trials (repeats)
Shutdown
Bpod
PC
Raspberry Pi
Settings used to set up data structure. Standby.
ready-signal
settings transmitted
start experiment
Transmit settings and wait.
All elements ready.
settings transmitted
ready-signal
Settings used to initialize treadmill input, tube and screen output.
Set up recording and state matrix.
Start new trial
transmit state matrix
go-signal
Set up recording and state matrix.
Send go signal to Bpod.
continous syncing of treadmill input/virtual output
See below
Send records from this trial to pc.
Bpod records
Combine records. (own, Bpod, Raspi)
Next trial. (Repeat)
Last trial.
movement/output records
Send records to pc.
continue sync
Shutdown Bpod.
stop-signal
Stop recording. Send stop-signal. Wait.
Raspberry Pi is shut down.
Process recordings?
end experiment
stop-signal
shutdow n confirmation
Shut down controls and virtual output. End all processes.
Communication during Trials
Bpod
PC
Raspberry Pi
new trial
Marker for trial start is sent out.
trial continues
Trigger causes reward state to be activated.
mouse...
...doesn't lick
...licks
Reward is dispensed.
Trial ends...
new trial
...by abort (fleeing).
...by timeout.
start marker
rew ard marker
Recording start.
Marker written to camera and microphone records.
Marker written to camera and microphone records.
Recordings stopped. Processing during intertrial.
timeout trigger
abort trigger
Trial abort written.
Timeout written.
positional trigger
Control of tube movement by treadmill enabled.
trial continues
Tube arrives at mouse.
if mouse flees
Trial abort sent out.
Timeout received.
Tube moved to starting position. Records sent to pc.
continous synchronization of visual movement context on screens to treadmill input, recording movement

4.3.2 The experiment is a series of trials, which are identical in their flow. They have a single initialization and shutdown phase (**Figure 12**). During the initialization, the settings that had been used earlier are transmitted by the PC workstation to the Raspberry Pi and Bpod. A confirmation of the handshake between the two is necessary before proceeding. This interaction places the Raspberry Pi in the virtual movement context, which remains active throughout the entire experiment. The handshake serves to trigger the workstation to transfer the state matrix to the state machine and send a go-signal, which causes the Bpod to start the trial.

4.3.3 The variables used in the trials can be divided into those that control the flow of the states and those that control the functional aspects of the setup. The state machine receives a state matrix build from the state lengths in the settings and then proceeds to run through this provided state matrix (**Figure 14**). This process is repeated for a set number of trials (decided by the experimenter) or alternatively the experimenter can control the process duration.

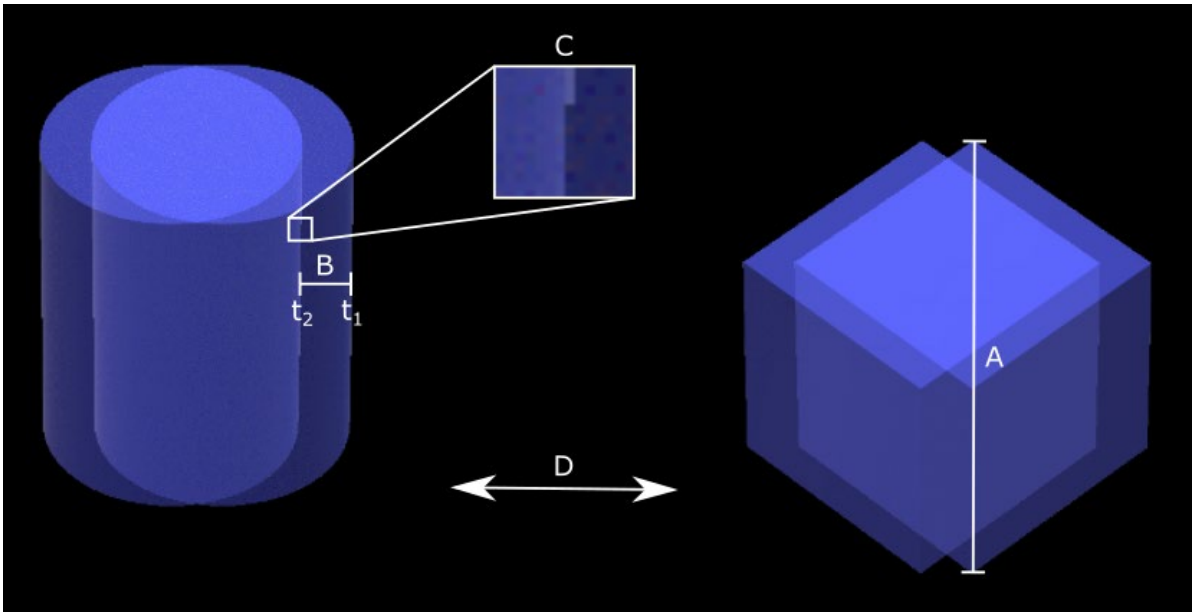

Figure 13 *Schematic showing the parameters of the virtual movement context.*
A) Height of the generated markers can be set in centimeters. **B**) Translation of the treadmill movement to the markers can be modified by a factor, making the context either more or less sensitive to the movement of the mouse. **C**) Resolution of the virtual context can be set as a multiple of the screen resolution, which allows for a faster drawing of the frames and thus a higher framerate, if desired. **D**) Movement direction of the virtual context can be set as a Boolean value, which indicates in which direction the positive side of the movement lies.

The other settings in the interface describe the processes in the virtual movement context (**Figure 13**) and tube movement, with some of them influencing both. This is required since it is intended to simulate the screens and tube as a combined, real environment. As described in the implementation on the Raspberry Pi, the same factor is applied when calculating the speed of the markers shown on the screen and the speed of the tube. Other factors only influence one of the two components. The size of the markers, the positive movement direction on the screens (which is dependent on the orientation of the screens), and the scaling of the resolution all influence solely the simulated visual context.

The detection of a fleeing mouse after the full approach to the tube is defined by the reward abort value, which corresponds to a percentage of the distance between the farthest position of the tube and the end position directly in front of the mouse, which the mouse has to move backwards, before the trial is aborted by the Raspberry Pi and the tube is reset to its original position.

One the next page:
Figure 14 *State matrix flowchart for every trial.*
The state matrix originates in state S1, which initiates the trial on the other elements by sending a start-byte. Its length is determined in the settings. It contains the wait time, the duration of time that the Bpod waits for a positional trigger from the Raspberry Pi. This sets the duration till a timeout in state S6 (failure state type 1/failure to approach). Should the positional trigger arrive in time, then state S2 will be reached and the Bpod will wait for a licking signal on the light-gated licking spout. This duration too will be determined in the settings. When the mouse licks in time, then the reward will be dispensed in state S3, which has the duration which is needed to open the reward solenoid long enough for the previously set reward amount to be dispensed. Should the mouse fail to lick in time, then the timeout will lead to state S7 (failure state type 2/failure to lick in time), or should the Raspberry Pi send a abort trigger during S2, then the trial will end in state S8 (failure state type 3/fleeing). The dispensing state S3 will transfer after its end to S4, which is a period during which the mouse can consume the reward and whose length is also determined in the settings. Should the Raspberry Pi send an abort trigger during this state, then it will transfer to S8 and the trial will end. If the state times out regularly, then state S5 will be reached and an exit-signal will be sent to the other components. The trial is considered a success at this point and a failed trial at all other exit-points. Adapted from original design by Lukas Kiwitz.

Figure 15 *Decision flowchart of a single trial.*
This will repeat after the inter-trial period if there are still trials left.

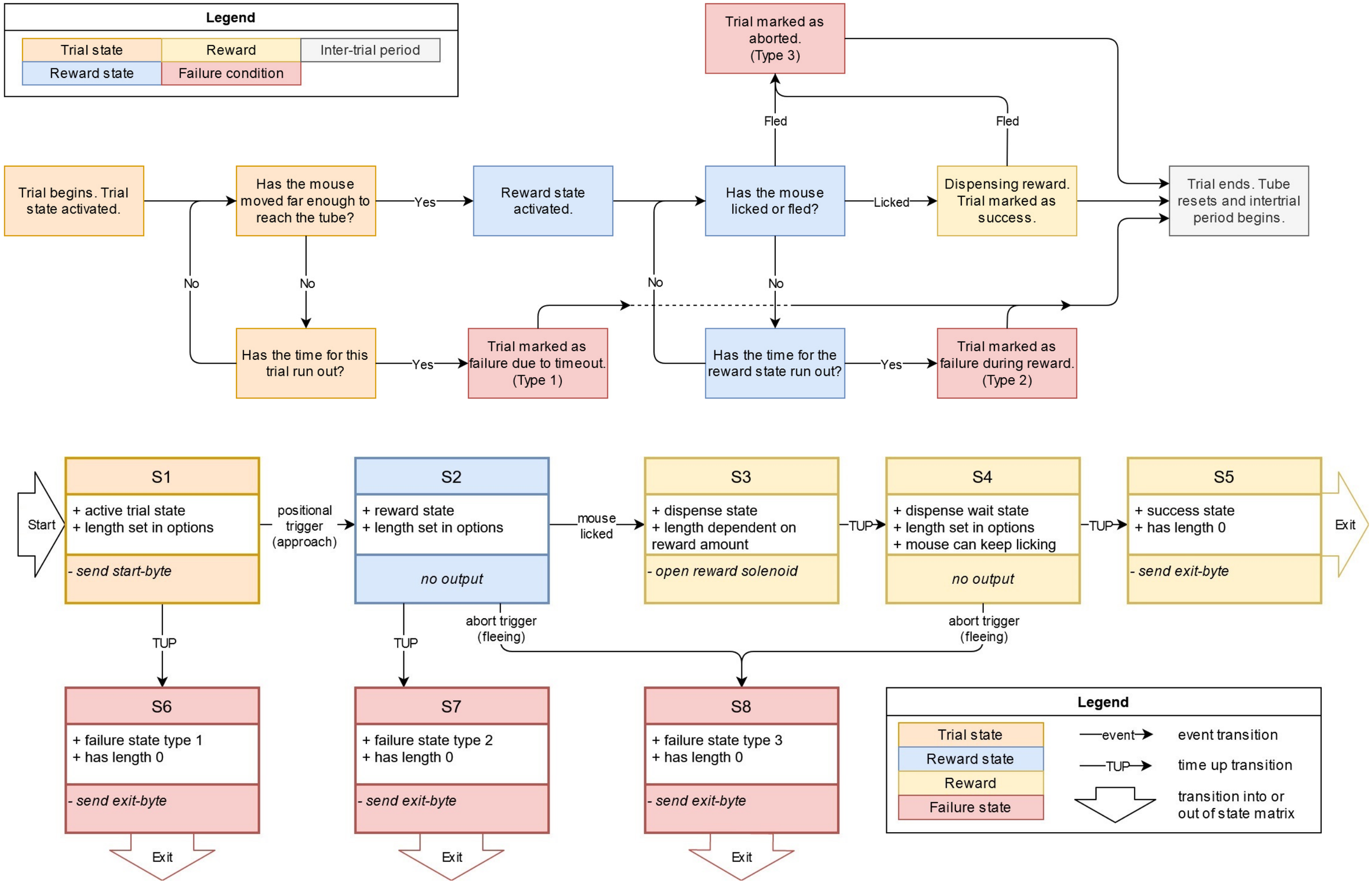
Legend
Trial state
Reward
Inter-trial period
Reward state
Failure condition
Trial begins. Trial state activated.
Has the mouse moved far enough to reach the tube?
Yes
Reward state activated.
Has the mouse licked or fled?
Licked
Dispensing reward. Trial marked as success.
Trial marked as aborted. (Type 3)
Fled
Fled
Trial ends. Tube resets and intertrial period begins.
No
No
No
No
Has the time for this trial run out?
Yes
Trial marked as failure due to timeout. (Type 1)
Has the time for the reward state run out?
Yes
Trial marked as failure during reward. (Type 2)
Start
S1
+ active trial state
+ length set in options
- send start-byte
positional trigger (approach)
S2
+ reward state
+ length set in options
no output
mouse licked
S3
+ dispense state
+ length dependent on reward amount
- open reward solenoid
TUP
S4
+ dispense wait state
+ length set in options
+ mouse can keep licking
no output
TUP
S5
+ success state
+ has length 0
- send exit-byte
Exit
TUP
TUP
abort trigger (fleeing)
abort trigger (fleeing)
S6
+ failure state type 1
+ has length 0
- send exit-byte
Exit
S7
+ failure state type 2
+ has length 0
- send exit-byte
Exit
S8
+ failure state type 3
+ has length 0
- send exit-byte
Exit
Legend
Trial state
Reward state
Reward
Failure state
event
event transition
TUP
time up transition
transition into or out of state matrix

4.3.4 The trials are structured identically and are determined by the configuration input into the settings. There are two distinct states in each trial: The main trial state, which means that the Bpod will wait for the signal from the Raspberry Pi that the mouse has moved to the tube, and the reward state, in which the Bpod waits for a licking input on the waterspout (**Figure 15**). Both states can encounter a timeout if the expected signal is not received in the time limit provided in the configuration. The reward state can additionally end if the Raspberry Pi sends an abort signal, if the mouse should decide to flee while it is at the tube. Timeouts and fleeing are both defined as missed trials.

Each of these missed trials is defined by a unique input or characteristic: Missed trials of type 1 are caused by a too slow approach or inactivity, which results in the failure to reach the tube in the limited time of the trial. This is a timeout of the trial state. Type 2 missed trials are caused by the mouse not licking at the licking spout quickly enough once it has reached the tube, which results in a timeout of the reward state. Finally, type 3 missed trials are marked by an abort of the trial, due to the mouse fleeing from the tube after having approached it.

If the mouse is successful, then the setup will assume a short waiting state, where the mouse will receive its reward, before the trial will end and the inter-trial period begins. Should the mouse flee during this reward reception period, then the trial will end the same way as it would during flight in the reward state. There is no high incidence of this situation expected, yet it can still be identified from the records of the Bpod state machine.

If there are still trials to run or time for the experiment left, the inter-trial period will lead to another trial. During the inter-trial period, the desktop computer receives the records from the Bpod upon exit of the last state and from the Raspberry Pi once it has received the timeout signal from the Bpod. The records and audio- and video-recordings are stored and will be processed later. Should all trials have finished or the time for the experiment has run out, then the experiment will end.

4.3.5 At the end of the experiment the mouse will be removed from the setup and returned to its holding cage. Then the virtual movement context will be terminated from the desktop interface and, optionally, the Raspberry Pi can be powered down by closing the application. The Bpod is controlled by the workstation and will not need its own power down sequence. After the application is closed, the setup will remain immobile and the rat can be removed from the tube and returned to its cage. Now the researcher can either continue to process the collected data with tools available on the desktop computer or power it down, too, and finally cut the power to the setup, ending the experiment session.

5. Experimental Applications

The setup described here can be used for research into natural threat perception. By introducing an innately threatening stimulus, we assess naturally occurring behaviors that are critical for the survival of the mouse. We assess neural circuits that evolved over the course of centuries, and that are probably conserved across species. These circuits are designed to detect threats, and to guide decision-making. Flight, fight and freezing behaviors have been observed in a variety of paradigms (Branco and Redgrave 2020), but which brain circuits are used to detect and to react to a threat are not completely understood. The rules behind the decision to run, freeze or continue foraging are not completely established. What pathways and processes are involved in the identification of, for example, a partially hidden rat? Which brain regions interact if the threat occurs during the search for a reward and which thresholds exist between a potential reward and threat? Our setup and experiment are intended to address these questions. Additional modifications to our current design, might involve the masking of the rat scent with a variety of odors or the combination of another mouse in the tube with the odor of a rat, which would allow the observation of behavior in similarly uncertain threat moments. It is also possible to introduce synthetic vocalizations and play them back to head restrained mice or to combine these and titrate the level of fear in the mouse. Additionally, it is possible to change how much of the rat is visible to mice, or to modify the virtual reality associated with the introduction or display of the threat. We could also modify or morph a variety of stimulus parameters to manipulate the perception of the mouse and thus achieve new insights into the influence of each perceptual sense on the recognition of a predator.

6. Conclusion

While designing and implementing this apparatus for studying the threat perception moment, it was necessary to consider many behavioral and design factors. We wanted the threat to be ambiguous, we wanted the interaction to generate innate fear in mice, and we wanted the threat to be multimodal. Here we settled on a mechanically straightforward combination of a treadmill that mice moved by walking, and a tube that was electronically linked to the movement of the treadmill. The tube moved toward the mouse when the mouse moved forward, and the tube moved away from the mouse when the mouse walked backward or when a trial had ended. The mobile tube had a dual purpose: it transported the lick spout for the mouse to obtain reward, and it contained a rat. Various aspects of the rat could be masked via a rotating disk: the mouse could see the rat, could smell the rat or could almost touch the rat. Not only was the design multimodal: odor, visual, and 3-dimensional visual stimuli were controlled; but it had a virtual visual component built into it. Throughout the experiment, multimodal data recorded from the treadmill can be combined with video observations of the details of mouse facial expression: pupil, whisker, and nose motion. In addition, the stepping motion of the animal, and the vocalizations of the mouse and rat can be recorded. The design that we have settled on is easily modifiable and can be used for imaging from the brain, from neurons in prefrontal and visual cortices, and from neurons in superficial and deep layers. Our goal is not just to understand the behavioral expression of the TPM, but the cognitive and neural circuits that are active and control the behavior of mice in recognizing fear, and in expressing fear. In its current design, elements can be easily added or modified. The optimal habituation and control parameters for moving the rat into position, or the number of trials in which a rat is presented to the mouse, still have to be determined. We do expect that the setup described here will be adaptable for future research into fear-based behavior.

Table of figures and tables

Code repository

The code developed for this setup can be found in a GitHub repository. It will be updated as the project progresses:

https://github.com/Marti-R/TPM.git

Table of used materials

Element	Vendor	Vendor-ID / GTIN	Comments	Amount
Desktop computer / Workstation				
Intel® Core i9-9900KF	Alternate GmbH	HN9I0002	CPU	1
GigaByte GeForce RTX 2080 Ti GAMING OC	Alternate GmbH	JHXY0R01	Graphics card	1
Corsair Force MP600 2TB	Alternate GmbH	IMLM5X04	NVMe SSD drive	1
Thermaltake Toughpower GF1 ARGB 850W	Alternate GmbH	TN8T31	Power supply unit	1
MSI MPG Z390 GAMING EDGE AC	Alternate GmbH	GNEM54	Mainboard	1
Be quiet! Dark Rock Slim	Alternate GmbH	HXLVBO	CPU-cooler	1
Corsair DIMM 32GB DDR4-3200 Kit	Alternate GmbH	IFIG5U22	Working memory	1
Corsair Carbide 200R	Alternate GmbH	TQXV6P	Tower chassis	1
Acer SB220Q Zero Frame Monitor	Amazon.com, Inc.	B07CVL2D2S	Full HD, 21.5” monitor for workstation	
Cherry WhisperKey Economy Keyboard	Amazon.com, Inc.	B00KF5UQPY	USB-Keyboard with QWERTY-layout	1
Logitech B100 Optical Mouse	Amazon.com, Inc.	B00AZKNPZC	3-button, black optical mouse	1
Control elements				
Bpod State Machine r2	Sanworks LLC	1024	Open control system for precision animal behavior measurement, comes with a 12V power supply	1
Analog input module 8ch	Sanworks LLC	1021	Analog input for Bpod; logging, streaming and event detection	1
Bpod Raspberry Pi Shim	Sanworks LLC	1031	Bpod & Raspberry Pi UART-interface, ‘shim’ form factor	1
Raspberry Pi 4 B 8GB All-In-Bundle	reichelt elektronik GmbH & Co. KG	RPI 4B 8GB ALLIN	Small, dual-display, desktop computer, comes with power supply, housing, microSD-card, cooling elements, and a microHDMI / HDMI-cable	1

ADS1115 ADC	Adafruit Industries	1085	16-bit, 4 channel analog-digital-converter	1
Arduino Nano	Arduino	7630049200173	Single-board microcontroller	1
SilentStepStick TMC2100	Watterott electronic GmbH	20150007	Stepper motor driver used to control the stepper motors for tube and disk	2
Philips 68.6” Monitor	Amazon Europe Core S.à r.l.	B00DPFM15Y	Full HD, 68.6” widescreen-monitor used to show the virtual movement context	2
GRS 3FR-4 Full Range Speaker	Amazon Europe Core S.à r.l.	B00K2ESJZ2	Full Range 3” Speaker Driver, 4 Ohm	1
Red light-emitting diode (LED)	Amazon Europe Core S.à r.l.	B002NL7PDE	Red LED with diffuse round lens, 2V	1
Snap-Action Switch with 16.7mm Lever	Pololu Corporation	1402	Single pole, double throw switch used to initialize the beginning and end of the tube’s movement range	2
Recording elements				
Basler ace acA1920-155uc Area Scan Camera	Basler AG	106880	Color camera which records a full body image of the mouse and a smaller region including its facial expressions	1
Basler ace acA1300-200um Area Scan Camera	Basler AG	106752	Monochromatic camera which is used to record and track the movement of the mouse’s eye, and to record a full-body image of the rat in the tube	2
1” 25mm C-Mount Lens	Kowa Optimed Germany GmbH	LM25HC	Lens used with the acA1920-155uc camera to capture full body images	1
1/2” 6mm C-Mount Lens	Kowa Optimed Germany GmbH	LM6NCM	Lens used with one of the acA1300-200um cameras to capture a full-body image of the rat in the tube to determine position and behavior during the experiment	1

2/3” 50mm C-Mount Lens	Kowa Optimed Germany GmbH	LM50JC1MS	Lens used with one of the acA1300-200um cameras to capture images and track the movement of the mouse’s pupil and face	1
2.5 x 2.5 cm mirror	Amazon Europe Core S.à r.l.	B07C1G5RKJ	Small, rectangular mirror used with camera to track eye-movement	1
Ultramic 384K BLE	Dodotronic di Ivano Pelicella	UM384BLE	Ultrasonic microphone used to record vocalizations from the mouse and rat in the setup, 384kHz sampling rate, can detect frequencies to up to 190kHz	2
Infrared LED Array Light Source	Thorlabs, Inc.	LIU850A	850nm IR Light Source for pupil tracking	1
Mechanical elements				
Treadmill with output box	CWW (Workshop)	-	Treadmill with an ouput box, 5V analog velocity and position channel, diameter 20cm, custom-made	1
Tube	CWW (Workshop)	-	Tube made from red plexiglass, diameter 10cm, custom-made	1
Disk	CWW (Workshop)	-	Stimulus modulation disk, diameter 15cm, custom-made	1
2-way NC pinch valve	msscientific Chromatographie-Handel GmbH	075P2NC12-01S	Pinch valve used to control the flow of reward liquid to the mouse during the experiment	1
Connectors	CWW (Workshop)	-	Connects elements between tube, stepper motors, rail, and disk, created with a 3D-printer, custom-made	1

NEMA 17 Stepper Motor	Watterott electronic GmbH	201898	A stepper motor with 200 steps per full rotation. I = 1.7A	2
Rail	CWW (Workshop)	-	Rail construction carrying the tube and the attached stepper motors, contains a silent chain to move the tube along the rail, contains 3D-printed parts, custom-made	1
Central Vacuum Pump	-	-	Vacuum pump integrated into the laboratory, which provides vacuum via pipes to the individual rooms in the laboratory	1
Structural elements				
Aluminum Breadboard, 450mmx750mmx12.7mm	Thorlabs, Inc.	MB4575/M	Aluminum breadboard, M6 Taps	1
Flat Screen Monitor Support Bracket with Articulating Arm	Thorlabs, Inc.	PSY121	Mount for virtual context screen	2
Ø1.5" Mounting Post	Thorlabs, Inc.	P200/M	Post for mounting the screen support brackets, M6 Taps, L = 200 mm	6
Studded Pedestal Base Adapter	Thorlabs, Inc.	PB4/M	Base for Ø1.5” Mounting Posts, M6 x 1.0 Thread	6
Clamping Fork for Pedestal Base Adapter	Thorlabs, Inc.	PF175B	Fork which will hold the pedestal base adapter on the breadboard	6
Fixed Position Retainer	Thorlabs, Inc.	RSPC	Small bracket to mark intended location of the mounting post bases	6
Ø12.7 mm Optical Post, L = 300 mm	Thorlabs, Inc.	TR300/M	Thinner post used as scaffolding for cameras and other recording elements, M4 Setscrew, M6 Tap	5

Ø12.7 mm Optical Post, L = 75 mm	Thorlabs, Inc.	TR75/M	Thinner mounting post for cameras and other recording elements, M4 Setscrew, M6 Tap	4
Right-angle Clamp for Ø12.7 mm Optical Post	Thorlabs, Inc.	RA90/M	Right-angle Clamp used to connect the Ø12.7 mm Optical Posts	
Metric Screw Thread Adapter Kit	Thorlabs, Inc.	HW-KIT6/M	Thread adapter Kit used to connect the Ø12.7 mm optical posts to the Ø1.5" optical posts	1
Sinvitron 11” Camera Arm & Clamp	Amazon Europe Core S.à r.l.	B011769YUM	Arm and clamp for mounting cameras and microphones to tube and optical breadboard	3
SMALLRIG DSLR Rig	Amazon Europe Core S.à r.l.	B00855QK0Q	Clamp with threaded hole to mount elements to scaffolding	2
Mirror Mount	CWW (Workshop)	-	3D-printed mount for the mirror, movable in 2 axes, allows view on the mouse’s eye from above with the 2/3” 50mm C-Mount Lens	1
Headpost holder with screw	CWW (Workshop)	-	Rod with tapered end to connect to a headpost via a screw, L = 10cm	1
Headpost	CWW (Workshop)	-	Aluminum headpost which gets implanted on the skull of the mice, 1 per mouse required	>1
Silicon Select tubing	msscientific Chromatographie-Handel GmbH	10025-01S	Tubing used with the solenoid pinch valve to deliver reward to the mouse during the trial, L = 50’	1
Piebert Silicone Tubing	Amazon Europe Core S.à r.l.	B073H9TFNL	Clear elastic tubing to connect the tube to the vaccum port, ID = 6mm, OD = 9mm	1

Assorted elements				
VIPMOON Jumper Cable Wires	Amazon Europe Core S.à r.l.	B07BLRNTXW	Roll of wires for 40 jumper cables, used for crimping, L = 1 m	2
AZDelivery Mini Breadboards	Amazon Europe Core S.à r.l.	B07VFK5CRP	Breadboards used to connect jumper cables between Arduino and Raspberry Pi, 5 pcs.	1
Kwmobile BNC Terminators	Amazon Europe Core S.à r.l.	B07FXWMFBV	BNC-terminators to connect the BNC-outputs from the treadmill control box to the ADC, 5 pcs.	1
RJ45 Terminator	Amazon Europe Core S.à r.l.	B085NL7DTH	RJ45-terminators to connect one of the Bpod's behaviour ports to the reward solenoid pinch valve	1
KabelDirekt Patch Cable	Amazon Europe Core S.à r.l.	B01FHZNXXI	Patch cable for connections between the workstation, Bpod, and Raspberry Pi	3
USB/miniUSB Cable	Amazon Europe Core S.à r.l.	B00NH13S44	USB/miniUSB-cable to connect to and instruct the Arduino Nano from the workstation	1
High-speed HDMI-Cable	Amazon Europe Core S.à r.l.	B014I8SSD0	HDMI-cable required for all 3 screens	3
Techole HDMI Splitter 1 in 2 out	Amazon Europe Core S.à r.l.	B07DW2445X	HDMI splitter to split the virtual context put out from the Raspberry Pi to 2 screens	1
DC Power Supply for IR Light Source	Thorlabs, Inc.	LIU-PS	Power supply for eye-tracking IR light-source, 24 V	1
LEICKE Power Supply 12V	Amazon Europe Core S.à r.l.	B01CYK0LGG	Power supply for Arduino Nano and stepper motors, 12V 2.5A	1
Power cord	Amazon Europe Core S.à r.l.	B00AOAJ78M	Power cord, 3m, for 230V power to screens and workstation	4

Table 1 *Table of materials required for the construction of the setup.*

References

Bandelow, Borwin, and Sophie Michaelis. 2015. "Epidemiology of Anxiety Disorders in the 21st Century." *Clinical Research* 17 (3): 9.

Betley, J. Nicholas, Zhen Fang Huang Cao, Kimberly D. Ritola, and Scott M. Sternson. 2013. "Parallel, Redundant Circuit Organization for Homeostatic Control of Feeding Behavior." *Cell* 155 (6): 1337–50. https://doi.org/10.1016/j.cell.2013.11.002.

Blanchard, Robert J., and D.Caroline Blanchard. 1989. "Attack and Defense in Rodents as Ethoexperimental Models for the Study of Emotion." *Progress in Neuro-Psychopharmacology and Biological Psychiatry* 13 (January): S3–14. https://doi.org/10.1016/0278-5846(89)90105-X.

Blanchard, Robert J, Mark A Hebert, Pier Ferrari, Paola Palanza, Rayson Figueira, D.Caroline Blanchard, and Stefano Parmigiani. 1998. "Defensive Behaviors in Wild and Laboratory (Swiss) Mice: The Mouse Defense Test Battery." *Physiology & Behavior* 65 (2): 201–9. https://doi.org/10.1016/S0031-9384(98)00012-2.

Branco, Tiago, and Peter Redgrave. 2020. "The Neural Basis of Escape Behavior in Vertebrates." *Annual Review of Neuroscience* 43 (1): annurev-neuro-100219-122527. https://doi.org/10.1146/annurev-neuro-100219-122527.

Breitbart, William. 2017. "Existential Guilt and the Fear of Death." *Palliative and Supportive Care* 15 (5): 509–12. https://doi.org/10.1017/S1478951517000797.

Castro, Daniel C., and Kent C. Berridge. 2017. "Opioid and Orexin Hedonic Hotspots in Rat Orbitofrontal Cortex and Insula." *Proceedings of the National Academy of Sciences* 114 (43): E9125–34. https://doi.org/10.1073/pnas.1705753114.

Cox, V. C., and E. S. Valenstein. 1965. "Attenuation of Aversive Properties of Peripheral Shock by Hypothalamic Stimulation." *Science* 149 (3681): 323–25. https://doi.org/10.1126/science.149.3681.323.

Dombeck, Daniel A, Christopher D Harvey, Lin Tian, Loren L Looger, and David W Tank. 2010. "Functional Imaging of Hippocampal Place Cells at Cellular Resolution during Virtual Navigation." *Nature Neuroscience* 13 (11): 1433–40. https://doi.org/10.1038/nn.2648.

Fanselow, Michael S. 1994. "Neural Organization of the Defensive Behavior System Responsible for Fear." *Psychonomic Bulletin & Review* 1 (4): 429–38. https://doi.org/10.3758/BF03210947.

Fanselow, Michael S., and Zachary T. Pennington. 2017. "The Danger of LeDoux and Pine's Two-System Framework for Fear." *American Journal of Psychiatry* 174 (11): 1120–21. https://doi.org/10.1176/appi.ajp.2017.17070818.

Flores, África, Miquel À. Fullana, Carles Soriano-Mas, and Raül Andero. 2018. "Lost in Translation: How to Upgrade Fear Memory Research." *Molecular Psychiatry* 23 (11): 2122–32. https://doi.org/10.1038/s41380-017-0006-0.

Foilb, Allison R., Johanna G. Flyer-Adams, Steven F. Maier, and John P. Christianson. 2016. "Posterior Insular Cortex Is Necessary for Conditioned Inhibition of Fear." *Neurobiology of Learning and Memory* 134 (October): 317–27. https://doi.org/10.1016/j.nlm.2016.08.004.

Gallagher, M, Pw Graham, and Pc Holland. 1990. "The Amygdala Central Nucleus and Appetitive Pavlovian Conditioning: Lesions Impair One Class of Conditioned Behavior." *The Journal of Neuroscience* 10 (6): 1906–11. https://doi.org/10.1523/JNEUROSCI.10-06-01906.1990.

Gehrlach, Daniel A., Nejc Dolensek, Alexandra S. Klein, Ritu Roy Chowdhury, Arthur Matthys, Michaela Junghänel, Thomas N. Gaitanos, et al. 2019. "Aversive State Processing in the Posterior Insular Cortex." *Nature Neuroscience* 22 (9): 1424–37. https://doi.org/10.1038/s41593-019-0469-1.

Ghazanfar, Asif A, John G Neuhoff, and Nikos K Logothetis. 2002. "Auditory Looming Perception in Rhesus Monkeys." *Proceeding of the National Academy of Sciences* 99 (24): 15755–57. https://doi.org/10.1073/pnas.242469699.

Gross, Cornelius T., and Newton Sabino Canteras. 2012. "The Many Paths to Fear." *Nature Reviews Neuroscience* 13 (9): 651–58. https://doi.org/10.1038/nrn3301.

Harvey, Christopher D., Forrest Collman, Daniel A. Dombeck, and David W. Tank. 2009. “Intracellular Dynamics of Hippocampal Place Cells during Virtual Navigation.” *Nature* 461 (7266): 941–46. https://doi.org/10.1038/nature08499.

Isogai, Yoh, Sheng Si, Lorena Pont-Lezica, Taralyn Tan, Vikrant Kapoor, Venkatesh N. Murthy, and Catherine Dulac. 2011. “Molecular Organization of Vomeronasal Chemoreception.” *Nature* 478 (7368): 241–45. https://doi.org/10.1038/nature10437.

Isosaka, Tomoko, Tomohiko Matsuo, Takashi Yamaguchi, Kazuo Funabiki, Shigetada Nakanishi, Reiko Kobayakawa, and Ko Kobayakawa. 2015. “Htr2a-Expressing Cells in the Central Amygdala Control the Hierarchy between Innate and Learned Fear.” *Cell* 163 (5): 1153–64. https://doi.org/10.1016/j.cell.2015.10.047.

Kanwar, Amrit, Shaista Malik, Larry J. Prokop, Leslie A. Sim, David Feldstein, Zhen Wang, and M. Hassan Murad. 2013. “THE ASSOCIATION BETWEEN ANXIETY DISORDERS AND SUICIDAL BEHAVIORS: A SYSTEMATIC REVIEW AND META-ANALYSIS: Research Article: Association Between Anxiety and Suicide.” *Depression and Anxiety*, February, n/a-n/a. https://doi.org/10.1002/da.22074.

Karli, P. 1956. “The Norway Rat’s Killing Response to the White Mouse: An Experimental Analysis.” *Behaviour* 10 (1/2): 81–103. https://doi.org/10.1163/156853956X00110.

Kawashima, Chiwa, Yoshihiro Tanaka, Ayako Inoue, Mari Nakanishi, Kana Okamoto, Yoshihiro Maruyama, Harumi Oshita, et al. 2016. “Hyperfunction of Left Lateral Prefrontal Cortex and Automatic Thoughts in Social Anxiety Disorder: A near-Infrared Spectroscopy Study.” *Journal of Affective Disorders* 206 (December): 256–60. https://doi.org/10.1016/j.jad.2016.07.028.

Kenney, Justin W., Ian C. Scott, Sheena A. Josselyn, and Paul W. Frankland. 2017. “Contextual Fear Conditioning in Zebrafish.” *Learning & Memory* 24 (10): 516–23. https://doi.org/10.1101/lm.045690.117.

Kessler, Ronald C., Maria Petukhova, Nancy A. Sampson, Alan M Zaslavsky, and Hans-Ullrich Wittchen. 2012. “Twelve-Month and Lifetime Prevalence and Lifetime Morbid Risk of Anxiety and Mood Disorders in the United States: Anxiety and Mood Disorders in the United States.” *International Journal of Methods in Psychiatric Research* 21 (3): 169–84. https://doi.org/10.1002/mpr.1359.

Krabbe, Sabine, Jan Gründemann, and Andreas Lüthi. 2018. “Amygdala Inhibitory Circuits Regulate Associative Fear Conditioning.” *Biological Psychiatry* 83 (10): 800–809. https://doi.org/10.1016/j.biopsych.2017.10.006.

LeDoux, Joseph E. 2014. “Coming to Terms with Fear.” *Proceedings of the National Academy of Sciences* 111 (8): 2871–78. https://doi.org/10.1073/pnas.1400335111.

LeDoux, Joseph E., and Richard Brown. 2017. “A Higher-Order Theory of Emotional Consciousness.” *Proceedings of the National Academy of Sciences* 114 (10): E2016–25. https://doi.org/10.1073/pnas.1619316114.

Logothetis, Nikos K, Jon Pauls, Mark Augath, Torsten Trinath, and Axel Oeltermann. 2001. “Neurophysiological Investigation of the Basis of the FMRI Signal” 412: 8.

Lonowski, Daniel J., Robert A. Levitt, and Scott D. Larson. 1973. “Mouse Killing or Carrying by Male and Female Long-Evans Hooded Rats.” *Bulletin of the Psychonomic Society* 1 (5): 349–51. https://doi.org/10.3758/BF03334368.

Mobbs, Dean, Ralph Adolphs, Michael S. Fanselow, Lisa Feldman Barrett, Joseph E. LeDoux, Kerry Ressler, and Kay M. Tye. 2019. “Viewpoints: Approaches to Defining and Investigating Fear.” *Nature Neuroscience* 22 (8): 1205–16. https://doi.org/10.1038/s41593-019-0456-6.

Molina, A. Fernandez de, and R. W. Hunsperger. 1959. “Central Representation of Affective Reactions in Forebrain and Brain Stem: Electrical Stimulation of Amygdala, Stria Terminalis, and Adjacent Structures.” *The Journal of Physiology* 145 (2): 251–65. https://doi.org/10.1113/jphysiol.1959.sp006140.

Mowrer, O. H., and R. R. Lamoreaux. 1946. “Fear as an Intervening Variable in Avoidance Conditioning.” *Journal of Comparative Psychology* 39 (1): 29–50. https://doi.org/10.1037/h0060150.

Nashaat, Mostafa A., Hatem Oraby, Robert N. S. Sachdev, York Winter, and Matthew E. Larkum. 2016. "Air-Track: A Real-World Floating Environment for Active Sensing in Head-Fixed Mice." *Journal of Neurophysiology* 116 (4): 1542–53. https://doi.org/10.1152/jn.00088.2016.

Neimeyer, Robert A., and Kenneth M. Chapman. 1981. "Self/Ideal Discrepancy and Fear of Death: The Test of an Existential Hypothesis." *OMEGA - Journal of Death and Dying* 11 (3): 233–40. https://doi.org/10.2190/62JN-TB4X-1H5F-HBC0.

Neumann, Inga D., and David A. Slattery. 2016. "Oxytocin in General Anxiety and Social Fear: A Translational Approach." *Biological Psychiatry* 79 (3): 213–21. https://doi.org/10.1016/j.biopsych.2015.06.004.

Panksepp, Jaak. 1971. "Aggression Elicited by Electrical Stimulation of the Hypothalamus in Albino Rats." *Physiology & Behavior* 6 (4): 321–29. https://doi.org/10.1016/0031-9384(71)90163-6.

Peng, Yueqing, Sarah Gillis-Smith, Hao Jin, Dimitri Tränkner, Nicholas J. P. Ryba, and Charles S. Zuker. 2015. "Sweet and Bitter Taste in the Brain of Awake Behaving Animals." *Nature* 527 (7579): 512–15. https://doi.org/10.1038/nature15763.

Perusini, Jennifer N., and Michael S. Fanselow. 2015. "Neurobehavioral Perspectives on the Distinction between Fear and Anxiety." *Learning & Memory* 22 (9): 417–25. https://doi.org/10.1101/lm.039180.115.

Phillips, R G, and Joseph E. LeDoux. 1992. "Differential Contribution of Amygdala and Hippocampus to Cued and Contextual Fear Conditioning." *Behavioral Neuroscience* 106 (2): 274–85. https://doi.org/10.1037//0735-7044.106.2.274.

Poort, Jasper, Adil G. Khan, Marius Pachitariu, Abdellatif Nemri, Ivana Orsolic, Julija Krupic, Marius Bauza, et al. 2015. "Learning Enhances Sensory and Multiple Non-Sensory Representations in Primary Visual Cortex." *Neuron* 86 (6): 1478–90. https://doi.org/10.1016/j.neuron.2015.05.037.

Renz, M., O. Reichmuth, D. Bueche, B. Traichel, M. Schuett Mao, T. Cerny, and F. Strasser. 2018. "Fear, Pain, Denial, and Spiritual Experiences in Dying Processes." *American Journal of Hospice and Palliative Medicine®* 35 (3): 478–91. https://doi.org/10.1177/1049909117725271.

Sakurai, Katsuyasu, Shengli Zhao, Jun Takatoh, Erica Rodriguez, Jinghao Lu, Andrew D. Leavitt, Min Fu, Bao-Xia Han, and Fan Wang. 2016. "Capturing and Manipulating Activated Neuronal Ensembles with CANE Delineates a Hypothalamic Social-Fear Circuit." *Neuron* 92 (4): 739–53. https://doi.org/10.1016/j.neuron.2016.10.015.

Schiff, Hillary C., Anna Lien Bouhuis, Kai Yu, Mario A. Penzo, Haohong Li, Miao He, and Bo Li. 2018. "An Insula–Central Amygdala Circuit for Guiding Tastant-Reinforced Choice Behavior." *The Journal of Neuroscience* 38 (6): 1418–29. https://doi.org/10.1523/JNEUROSCI.1773-17.2017.

Schiff, William. 1965. "Perception of Impending Collision: A Study of Visually Directed Avoidant Behavior." *Psychological Monographs: General and Applied* 79 (11): 1–26. https://doi.org/10.1037/h0093887.

Silva, Bianca A., Cornelius T. Gross, and Johannes Gräff. 2016. "The Neural Circuits of Innate Fear: Detection, Integration, Action, and Memorization." *Learning & Memory* 23 (10): 544–55. https://doi.org/10.1101/lm.042812.116.

Simon-Kutscher, Kathrin, Nadine Wanke, Carlo Hiller, and Lars Schwabe. 2019. "Fear Without Context: Acute Stress Modulates the Balance of Cue-Dependent and Contextual Fear Learning." *Psychological Science* 30 (8): 1123–35. https://doi.org/10.1177/0956797619852027.

Smith, D. E., M. B. King, and B. G. Hoebel. 1970. "Lateral Hypothalamic Control of Killing: Evidence for a Cholinoceptive Mechanism." *Science* 167 (3919): 900–901. https://doi.org/10.1126/science.167.3919.900.

Stowers, Lisa, and Tsung-Han Kuo. 2015. "Mammalian Pheromones: Emerging Properties and Mechanisms of Detection." *Current Opinion in Neurobiology* 34 (October): 103–9. https://doi.org/10.1016/j.conb.2015.02.005.

Stowers, Lisa, and Darren W Logan. 2010. “Olfactory Mechanisms of Stereotyped Behavior: On the Scent of Specialized Circuits.” *Current Opinion in Neurobiology* 20 (3): 274–80. https://doi.org/10.1016/j.conb.2010.02.013.

Takahashi, Lorey K., Megan M. Chan, and Mark L. Pilar. 2008. “Predator Odor Fear Conditioning: Current Perspectives and New Directions.” *Neuroscience & Biobehavioral Reviews* 32 (7): 1218–27. https://doi.org/10.1016/j.neubiorev.2008.06.001.

Toth, Iulia, and Inga D. Neumann. 2013. “Animal Models of Social Avoidance and Social Fear.” *Cell and Tissue Research* 354 (1): 107–18. https://doi.org/10.1007/s00441-013-1636-4.

Tovote, Philip, Jonathan Paul Fadok, and Andreas Lüthi. 2015. “Neuronal Circuits for Fear and Anxiety.” *Nature Reviews Neuroscience* 16 (6): 317–31. https://doi.org/10.1038/nrn3945.

Wittchen, H.U., F. Jacobi, J. Rehm, A. Gustavsson, M. Svensson, B. Jönsson, J. Olesen, et al. 2011. “The Size and Burden of Mental Disorders and Other Disorders of the Brain in Europe 2010.” *European Neuropsychopharmacology* 21 (9): 655–79. https://doi.org/10.1016/j.euroneuro.2011.07.018.

Xu, Haifeng, Ling Liu, Yuanyuan Tian, Jun Wang, Jie Li, Junqiang Zheng, Hongfei Zhao, et al. 2019. “A Disinhibitory Microcircuit Mediates Conditioned Social Fear in the Prefrontal Cortex.” *Neuron* 102 (3): 668-682.e5. https://doi.org/10.1016/j.neuron.2019.02.026.

Yang, William, Ton Staps, and Ellen Hijmans. 2010. “Existential Crisis and the Awareness of Dying: The Role of Meaning and Spirituality.” *OMEGA - Journal of Death and Dying* 61 (1): 53–69. https://doi.org/10.2190/OM.61.1.c.

Yilmaz, Melis, and Markus Meister. 2013. “Rapid Innate Defensive Responses of Mice to Looming Visual Stimuli.” *Current Biology* 23 (20): 2011–15. https://doi.org/10.1016/j.cub.2013.08.015.

Acknowledgements

I would like to thank Prof. Dr. Matthew Larkum for giving me the possibility to learn and work in his lab, and for giving me the equipment to develop this setup.

I also want to thank him and Prof. Dr. Michael Brecht for their time and attention spent reading and evaluating my master thesis.

I am grateful to Dr. Robert Sachdev for patiently guiding me in this project and helping me during the revision process of this thesis.

I also want to thank him and Prof. Dr. Panayiota Poirazi for their contributions to the design of this setup.

Furthermore, I want to thank…

Dr. Julia Ledderose and Anna Nasr, for their essential help with the initial LaGeSo-application.

Hatem Oraby, for his helpful ideas and suggestions for the control and synchronization of the recording components in the setup.

Eduardo Maristany, for providing his implementation of the camera triggers on the Bpod platform.

Jan-Erik Ode and Alexander Schill, for their work as part of the "Centrum Wissenschaftliche Werkstätten", the workshop of the Charité, in creating the prototype of the setup.

Ronny Bergmann, for designing and implementing the motor-control circuit and programming the Arduino Nano.

Lukas Kiwitz, for his contributions to the interface and Bpod code.

Lara Chirich, for her contributions to the currently running experiments, and for her help with handling and habituation of the rats and mice.

The members of the ERC Synergy working group, including Prof. Dr. Johannes Letzkus, Prof. Dr. Attila Losonczy, Prof. Dr. Matthew Larkum, and Prof. Dr. Panayiota Poirazi for their push to do this work.

All members of LarkumLab, for their part in providing a supportive and inspiring work environment.

Declaration of authenticity / Eigenständigkeitserklärung

Hiermit erkläre ich, dass ich die vorliegende Arbeit selbständig verfasst habe und sämtliche Quellen, einschließlich Internetquellen, die unverändert oder abgewandelt wiedergegeben werden, insbesondere Quellen für Texte, Grafiken, Tabellen und Bilder, als solche kenntlich gemacht habe.

Ich versichere, dass ich die vorliegende Abschlussarbeit noch nicht für andere Prüfungen eingereicht habe.

Mir ist bekannt, dass bei Verstößen gegen diese Grundsätze ein Verfahren wegen Täuschungsversuchs bzw. Täuschung gemäß der fachspezifischen Prüfungsordnung und/oder der Fächerübergreifenden Satzung zur Regelung von Zulassung, Studium und Prüfung der Humboldt-Universität zu Berlin (ZSP-HU) eingeleitet wird.

Berlin, den 05.09.2016 _ 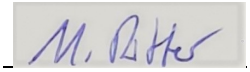

Marti Ritter